

Glial Differentiation Of Human Umbilical Stem Cells In 2d And 3d Environments

2011

Hedvika Davis
University of Central Florida

Find similar works at: <https://stars.library.ucf.edu/etd>

University of Central Florida Libraries <http://library.ucf.edu>

STARS Citation

Davis, Hedvika, "Glial Differentiation Of Human Umbilical Stem Cells In 2d And 3d Environments" (2011). *Electronic Theses and Dissertations*. 2028.

<https://stars.library.ucf.edu/etd/2028>

This Doctoral Dissertation (Open Access) is brought to you for free and open access by STARS. It has been accepted for inclusion in Electronic Theses and Dissertations by an authorized administrator of STARS. For more information, please contact lee.dotson@ucf.edu.

GLIAL DIFFERENTIATION OF HUMAN UMBILICAL STEM
CELLS IN 2D AND 3D ENVIRONMENTS

by
HEDVIKA DAVIS
M.S. University of Central Florida, 2002

A dissertation submitted in partial fulfillment of the requirements
for the degree of Doctor of Philosophy in Biomedical Sciences
in the Burnett School of Biomedical Sciences
in the College of Medicine
at the University of Central Florida,
Orlando, Florida

Spring Term 2011
Major Professor: James J. Hickman

ABSTRACT

During differentiation stem cells are exposed to a range of microenvironmental chemical and physical cues. In this study, human multipotent progenitor cells (hMLPCs) were differentiated from umbilical cord into oligodendrocytes and astrocytes. Chemical cues were represented by a novel defined differentiation medium containing the neurotransmitter norepinephrine (NE). In traditional 2 dimensional (2D) conditions, the hMLPCs differentiated into oligodendrocyte precursors, but did not progress further. However, in a constructed 3 dimensional (3D) environment, the hMLPCs differentiated into committed oligodendrocytes that expressed MBP. When co-cultured with rat embryonic hippocampal neurons (EHNs), hMLPCs developed in astrocytes or oligodendrocytes, based on presence of growth factors in the differentiation medium. In co-culture, physical cues provided by axons were essential for complete differentiation of both astrocytes and oligodendrocytes. This study presents a novel method of obtaining glia from human MLPCs that could eliminate many of the difficulties associated with their differentiation from embryonic stem cells. In addition, it reveals the complex interplay between physical cues and biomolecules on stem cell differentiation.

ACKNOWLEDGMENTS

This dissertation would not have been possible without help of many special people. I would like to express my deepest appreciation and gratitude to my advisor and committee chair, Dr. James J. Hickman for providing me with guidance and support, for his kindness and most of all, for his patience. His wide knowledge, understanding and his logical way of thinking have been of great value and inspiration for me. I gratefully acknowledge the committee member Dr. Stephen Lambert for his professional advice and supervision during this study. I have benefited greatly from his wisdom, valuable inputs and originality. I would also like to thank the committee members Dr. Peter Molnar, Dr. Pappachan E. Kolattukudy and Dr. Kiminobu Sugaya for their assistance, expertise and constructive comments throughout this work. My research would not have been possible without their help. I extend my sincere gratitude to my co-workers and friends who have always kindly given me their time and were constant source of ideas. Finally, I owe my warmest regards to my family for their encouragement and support.

TABLE OF CONTENTS

LIST OF TABLES	viii
1. INTRODUCTION AND REVIEW OF THE LITERATURE	1
1.1. Oligodendrocytes: Historical Overview	1
1.2. Astrocytes: Rising Stars	3
1.3. Development of Oligodendrocytes and Astrocytes	5
1.4. Effect of Noradrenergic Signaling on Oligodendrocyte and Astrocyte Differentiation	9
1.5. Effect of Physical Cues on Differentiation	13
1.6. Differentiation of Human MLPCs from Umbilical Cord into Glia	14
2. MATERIALS AND METHODS	18
2.1. Modification of Surfaces	18
2.2. Patterns Preparation	18
2.3. Contact Angle Measurements	19
2.4. X-Ray Photoelectron Spectroscopy	20
2.5. hMLPCs Cell Culture	22
2.6. EHNs Cell Culture	22
2.7. Induction of Oligodendrocyte Differentiation	23
2.8. Co-cultures	24
2.9. Construction of 3D Environment	24
2.10. Morphological Analysis	25
2.11. Immunocytochemistry	25
2.12. Isolation of Astrocytes by Discontinuous Percoll Gradients	26

2.13. Quantification	27
3. RESULTS	28
3.1 Acquisition of Neuronal Morphology	28
3.2. Transient Expression of Neuronal Markers	30
3.3. hMLPCs and Oligodendrocytes May Share Neuroepithelial Origin	33
3.4. Differentiation of hMLPCs in a 2D Environment	35
3.5. Differentiation of hMLPCs in a 3D Environment	41
3.6. hMLPCs Express Functional ARs in the 3D System	48
3.7. Activation of Both α - and β -AR is Essential for Differentiation in the 3D System	51
3.8. Co-culture of hMLPC with EHNs	55
3.9. Differentiating Human Oligodendrocytes can be distinguished from Rat Neurons	59
3.10. hMLPCs Differentiate into Mature Oligodendrocytes in the Presence of EHNs	62
3.11. Differentiated Oligodendrocytes Wrap around Axons in Culture	66
3.12 Generation of Pure Astrocyte Population	68
4. DISCUSSION	70
LIST OF REFERENCES	77

LIST OF FIGURES

Figure 1. Oligodendrocytes.	2
Figure 2. Electron Micrograph Image. Branched Oligodendrocytes with Processes Extending to Underlying Axons (http://www.regenecell.com).	2
Figure 3. Glia-neuron interaction.	4
Figure 4. Sequential Model.	5
Figure 5. Diagram Depicting the Differentiation of the O2A Lineage.	8
Figure 6. Molecular Structure of Norepinephrine.	10
Figure 7. Schematic Representation of the Cortical Noradrenergic Afferents with Neuronal, Vascular and Glial Elements.	11
Figure 8. Electron Micrographs of Oligodendroglial Perikarya.	11
Figure 9. Norepinephrine Acts on its Target Cells by Binding to and Activating Alpha and Beta-Adrenergic Receptors (ARs).	12
Figure 10. Schematic Illustration of the Role of Cell Shape and Cytoskeletal Tension in the Differentiation of MSCs.	14
Figure 11. XPS Analysis of a DETA modified of Glass Coverslip.	21
Figure 12. Phase Images of hMLPCs Treated with 100 μ M NE for 4 hrs.	29

Figure 13. Transient Expression of Motoneuron Markers 17 hrs after Treatment with 100 μ M NE.	31
Figure 14. Immunocytochemical Analysis of Untreated hMLPC Suggest Neuroepithelial Origin.	34
Figure 15. Phase Contrast Images of Differentiating hMLPCs in 2D Environment.	37
Figure 16. 2D Environment Promotes Differentiation of hMLPCs along Early Stages of Oligodendroglial Lineage.	39
Figure 17. 3D Environment Promotes Further Differentiation of hMLPCs.	42
Figure 18. hMLPCs Differentiate into Committed Oligodendrocytes in a 3D Environment.	44
Figure 19. Expression of α 1- and β 1-ARs.	49
Figure 20. Influence of ARs on Differentiation of hMLPCs into Oligodendrocytes.	53
Figure 21. Morphological Changes of hMLPCs at 48 hrs after the Co-culture.	56
Figure 22. Phase Contrast Images of hMLPCs Co-cultured with EHNs.	58
Figure 23. Immunocytochemical Analysis Distinguished hMLPCs from Rat EHNs.	60
Figure 24. Immunocytochemical Analysis of Co-cultures Differentiated for 14 Days.	64
Figure 25. Immunocytochemical Analysis of Mature Oligodendrocytes.	67
Figure 26. Percoll Gradient Separation of Astrocytes ⁹⁷	68
Figure 27. Immunocytochemistry of Astrocytes Isolated by Percoll Gradient.	69

LIST OF TABLES

Table 1. Percentage of Cells Exhibiting Neuron-like Morphology in Response to NE.	30
Table 2. Percentage of Cells Exhibiting Oligodendroglial Morphology in Response to NE.	32
Table 3. Percentage of Cells Developing Processes in Response to Surface Modification.	47

LIST OF ABBREVIATIONS

ARs.....	Adrenergic Receptors
bFGF.....	Basic Fibroblast Growth Factor
β IIIIT.....	Beta III Tubulin
DETA.....	Trimethoxy-Silylpropyl-Diethylenetriamine
DMEM	Dulbecco's Modified Eagle Media
EGF.....	Epidermal Growth Factor
EHNs.....	Embryonic Hippocampal Neurons
FBS.....	Fetal Bovine Serum
HuNu.....	Human Specific Nuclear Antigen
MBP.....	Myelin Basic Protein
hMLPCs.....	Human Multi-Lineage Progenitor Cells
PDGF-AA.....	Platelet-Derived Growth Factor-AA
PEF.....	PDGF-AA+EGF+bFGF
PEG.....	Polyethyleneglycol
¹³ F.....	Fluorinated Silane

1. INTRODUCTION AND REVIEW OF THE LITERATURE

1.1. Oligodendrocytes: Historical Overview

Oligodendrocytes are glial cells in central nervous system (CNS). They were the last glial cells discovered at the beginning of the 20th century. These cells were resistant to classical metal impregnations used for staining cells. However, a new staining method created by Pio del Rio Hortega led him to visualize these cells in 1921. He introduced the word "oligodendrocyte" from the Greek -oligo- for few, -dendro- for tree, and -cyte- for cell, to describe a cell with fewer processes than the other cells. Oligodendrocytes make and maintain CNS myelin, the protective sheath around axons, referred to as white matter¹. The myelin sheath is a lipid rich membrane formed by modified extensions of oligodendroglial cell processes, wrapped in a spiral fashion around an axon². The word myelin originates from Greek myelos, meaning marrow. Myelin was named and described in 1858 by the German pathologist Rudolf Virchow because of its resemblance to marrow, long before its function or its composition was known. Each oligodendrocyte is able to myelinate as many as 50 different axons². The sections of myelin are separated from each other by small segments in which the bare axon is exposed to the interstitial space. These segments are called nodes of Ranvier, after the French histologist Louis-Antoine Ranvier who described them for the first time in 1878. Nodes of Ranvier are the location of multiple sodium channels. Along unmyelinated fibers, action potential moves continuously. However, when the axon is myelinated, the electrical impulse cannot flow through the high-resistance myelin sheath and therefore flows out through from one node of Ranvier to the next

node with little energy and increased speed. The non-linear and rapid conduction of electrical impulses is called saltatory conduction, because the action potential jumps from node to node³⁻⁵.

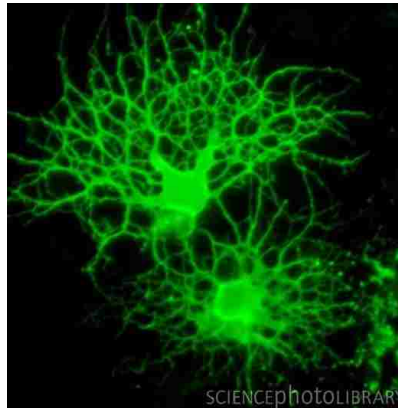


Figure 1. Oligodendrocytes.

Fluorescent light micrograph of oligodendrocytes from a mouse. The mouse had been genetically engineered to express green fluorescent protein (GFP) in its oligodendrocytes.



Figure 2. Electron Micrograph Image. Branched Oligodendrocytes with Processes Extending to Underlying Axons (<http://www.regenecell.com>).

1.2. Astrocytes: Rising Stars

Astrocytes are star-shaped glial cells. They are the most numerous cell type within the central nervous system (CNS), first identified at the 19th century by Von Lenhossek⁶. Until recently, astrocytes have been considered to be uninteresting ‘brain glue’, providing an inert scaffold and nutritional support necessary for neuronal distribution and interactions⁷. Recent findings suggest many new functions for these cells and highlight the importance of viewing most brain activities as collaboration between astrocytes and neurons. Astrocytes have been implicated in maintenance of the blood-brain barrier, dynamic regulation of neuron production, synaptic network formation and neuron electrical activity and in specific neurological diseases. This multi-functionality may explain the multiplicity of astrocyte subtypes found throughout the CNS. The human CNS has the highest numbers of glia, the greatest glia-neuron ratio⁸⁻¹⁰, and the greatest heterogeneity of glial cells¹¹ compared with other animal species. The broad category of astrocytes is subdivided into fibrous or protoplasmic subtypes, based on their morphology, antigen binding and localization to white or gray matter¹². Fibrous astrocytes have many glial filaments and are located mainly in white matter; protoplasmic astrocytes have fewer glial filaments and are found mainly in gray matter^{12, 13}. Whereas fibrous astrocytes tend to have regular contours and to extend cylindrical branching processes, protoplasmic astrocytes have irregular contours and extend sheet-like processes. Fibrous and protoplasmic astrocytes were suggested to be biochemically and developmentally distinct and correspond to the type-1 and type-2 astrocytes, originally defined in cultures of developing rat optic nerve^{12, 14}.

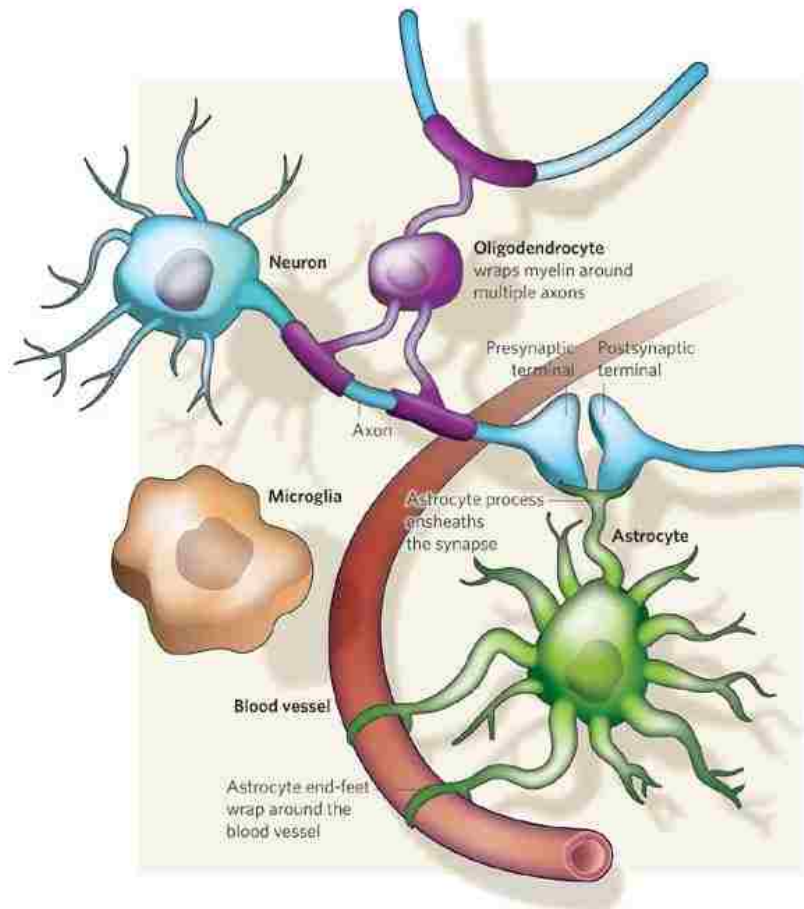


Figure 3. Glia-neuron interaction.

Different types of glia interact with neurons and the surrounding blood vessels. Oligodendrocytes wrap myelin around axons to speed up neuronal transmission. Astrocytes extend processes that ensheath blood vessels and synapses. Microglia keep the brain under surveillance for damage or infection¹⁵.

1.3. Development of Oligodendrocytes and Astrocytes

Oligodendrocytes and astrocytes arise from neuroepithelial stem cells early during development of brain and spinal cord. Neuroepithelial stem cells proliferate and give rise first to motoneuron and later to glial progenitor cells¹⁶⁻¹⁹. Some findings provide evidence that a common glial progenitor cell gives rise to both oligodendrocytes and astrocytes²⁰⁻²². Other findings suggest that oligodendrocytes either derive independently or derive from common motoneuron and oligodendrocyte precursors^{23, 24}. The most recent studies support a sequential model of differentiation (Figure3). In this model, motoneurons, oligodendrocytes and astrocytes arise sequentially from sequentially derived precursors²⁵.

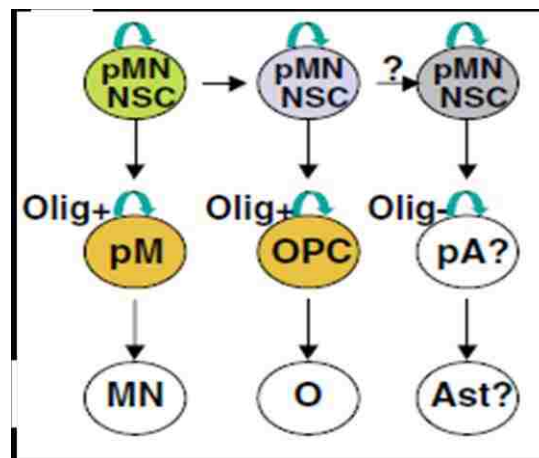


Figure 4. Sequential Model.

The sequential model explains how neuroepithelial stem cells (NSC) might generate motoneurons (MN), oligodendrocytes (O) and astrocytes (Ast) (pM, motoneuron precursor; OPC, oligodendrocyte precursor; pA, astrocyte precursor). NSCs at different stages in the sequential model are coded in different colors to reflect restrictions in competence²⁵.

The precursors are found in close contact with the surrounding environment that serves as a source of many chemical and biophysical signals. The signals from other cells and the extracellular environment are then integrated with the intracellular forces to control proper and timely differentiation²⁶. The early steps of differentiation can sometimes be reversed or altered when specific microenvironmental signals are absent or overridden²⁷. For example, bi-potential glial progenitor cells were shown to develop in vitro into a specific astrocyte population (the type-2 astrocyte) if cultured in presence of serum or into oligodendrocytes if cultured in the absence of serum²⁸. In certain culture conditions some of these cells acquire a mixed phenotype, displaying properties of both astrocytes and oligodendrocytes, or revert back to stem cell like cells. Due to its potential, the single glial progenitor cell is alternatively called an oligodendrocyte type-2 astrocyte (O2A) progenitor or an oligodendrocyte precursor cell (OPC)²⁹. O2As can be immunostained with the monoclonal antibody A2B5, which detects gangliosides on the surface of the cells³⁰.

The progression of the oligodendroglial lineage is characterized by dramatic morphological changes and the acquisition of specific surface antigens. The oligodendrocyte progenitors can be detected with the A2B5 antibody. Precursors express the O4 sulfatide, which persists in ramified but yet immature oligodendrocytes. Committed oligodendrocytes lose A2B5 reactivity after they begin to express O1 galactocerebroside. Differentiated oligodendrocytes, which are post-mitotic and richly multipolar cells, when mature, express myelin proteins such as myelin basic protein (MBP), and gradually initiate the process of myelination³⁰⁻³³.

Developing type-2 astrocytes exhibit radial processes and also express the gangliosides detected with the A2B5 antibody at early stages of differentiation. However, they are distinguished from

O2As by their expression of the astrocyte marker, glial fibrillary acidic protein (GFAP). As astrocytes mature, their GFAP expression remains, while A2B5 immunoreactivity diminishes. The type-2 astrocytes can be found in white but mainly in gray matter throughout the CNS^{12, 14}. They were observed in tracts of myelinated axons and there is evidence that processes from type-2 astrocytes contribute to the structure of nodes of Ranvier. They have been also shown to promote myelination in response to electrical impulses³⁴. It has been suggested that the O2A lineage is involved in construction of myelin sheaths and nodes in the mammalian CNS³⁵.

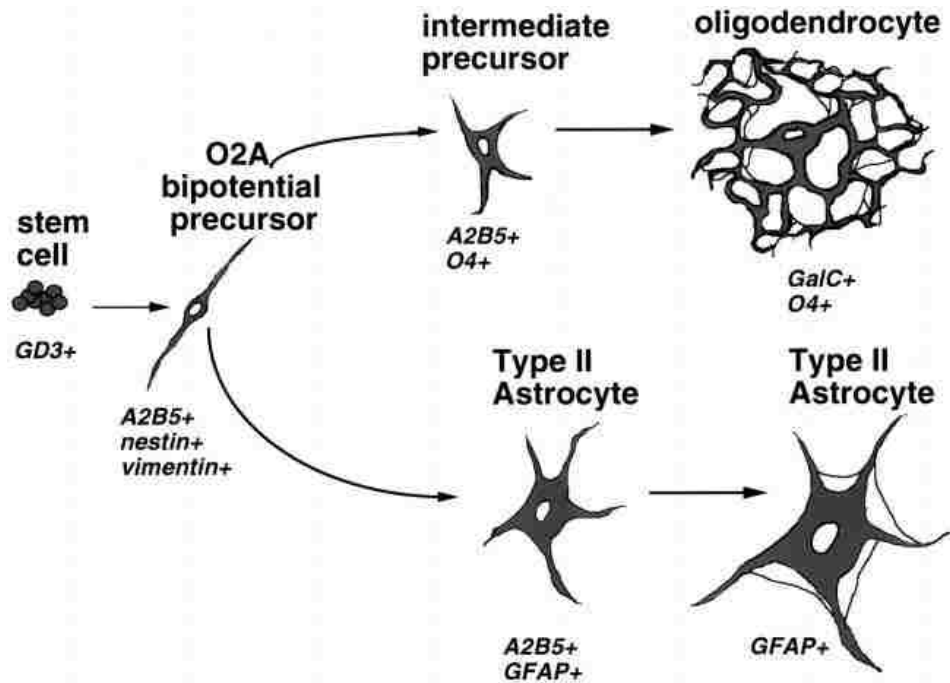


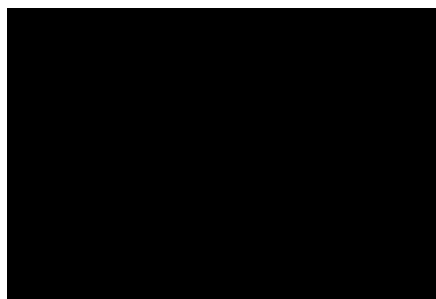
Figure 5. Diagram Depicting the Differentiation of the O2A Lineage.

The differentiation of oligodendrocytes from their progenitors follows a morphological transformation from a GD3 positive spherical stem cell to the A2B5 and nestin positive bipotential O2A precursor cell. When cultured in the presence of defined medium, the O2A precursors becomes a prooligodendrocyte, which is multipolar, has short processes, and exhibits immunoreactivity with the O4 antibody. The prooligodendrocyte differentiates into the galactocerebroside (GC or O1 antigen) positive oligodendrocyte. When the O2A precursor is cultured in the presence of serum, it differentiates into the A2B5¹ type 2 astrocyte, expressing GFAP. Type 2 astrocytes exhibit a stellate morphology³⁰.

1.4. Effect of Noradrenergic Signaling on Oligodendrocyte and Astrocyte Differentiation

Differentiation of oligodendrocytes and astrocytes in the local tissue environment depends closely on the gradients of soluble factors and physical cues activating distinct signaling pathways. The development to an oligodendrocytes phenotype is controlled by distinct molecular mechanisms. The soluble factors involve platelet-derived growth factor-AA (PDGF-AA), basic fibroblast growth factor (bFGF), epidermal growth factor (EGF) and changes in intracellular cyclic adenosine monophosphate (cAMP) levels. Another soluble factor involved in differentiation is norepinephrine (NE)³⁶⁻³⁹. NE is a small molecule catecholamine with a dual role as a hormone and a neurotransmitter. As a hormone, it is secreted by the adrenal gland and along with epinephrine it affects the fight or flight response during times of stress. As a neurotransmitter it is released from noradrenergic neurons and modulates emotions, learning and memory⁴⁰⁻⁴². NE has been shown to be involved in the development and functional maturation of spinal cord⁴³. The noradrenergic nerve terminals can be visualized in the ventral horn at birth, with a pattern similar to that of the adult, and regulate development of spinal motoneurons⁴³⁻⁴⁵. Previous studies demonstrated a function of NE in the neuronal differentiation of cells that express adrenergic receptors (ARs)^{46, 47}. The effect of NE on oligodendrocyte differentiation is not well understood. However, it was revealed that noradrenergic fibers contact oligodendrocytes at sites that resemble symmetrical synapses, suggesting that oligodendrocytes are NE's primary target⁴⁸. NE binds to and activates α and β - ARs. Oligodendrocytes express both α -1 and β - ARs^{37, 49-51}. It has also been shown that activation of α -1 adrenergic signaling influenced formation of processes and production of myelin. NE increases activity of protein kinase C (PKC), p38 mitogen-activated protein kinases (MAPK) and phosphoinositide (PI) hydrolysis^{49, 50}.

^{52, 53}. Alternatively, activation of β -adrenergic signaling by NE inhibits proliferation and accelerated lineage progression. The biological effect of NE is mediated through an increase in intracellular cAMP, activity of ERK (extracellular signal-regulated kinase) and of proteins essential for the cell cycle arrest. It was suggested that β -AR-mediated signaling may be restricted to proliferative phases of oligodendrocyte development, and dismantled after proliferation arrest^{37, 54, 55}.



4-[(1*R*)-2-amino-1-hydroxyethyl]benzene-1,2-diol

(C₈ H₁₁ N O₃)

Figure 6. Molecular Structure of Norepinephrine.

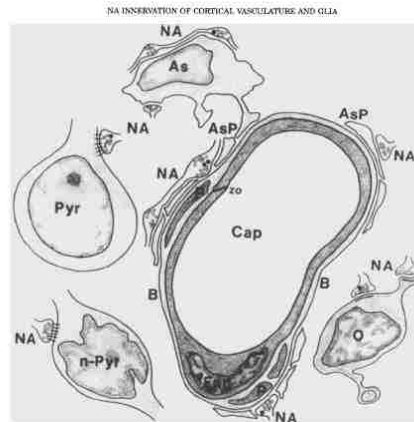


Figure 7. Schematic Representation of the Cortical Noradrenergic Afferents with Neuronal, Vascular and Glial Elements.

Pyramidal and non-pyramidal neurons have been shown to have noradrenergic synapses and astrocytes and oligodendrocytes are engaged in discrete anatomical relationships with noradrenergic boutons and fibers (As, astrocyte; ASP, astroglial processes; B, basal lamina; Cap, capillary; End, endothelial cell; NA, noradrenaline; n-Pyr, non-pyramidal neuron; O, oligodendrocyte; P, pericyte; Pyr, pyramidal neuron; zo, zonula occludens⁴⁸).



Figure 8. Electron Micrographs of Oligodendroglial Perikarya.

Arrowheads indicate thickening of the oligodendrocyte membrane at the site of contact with noradrenergic boutons⁴⁸.

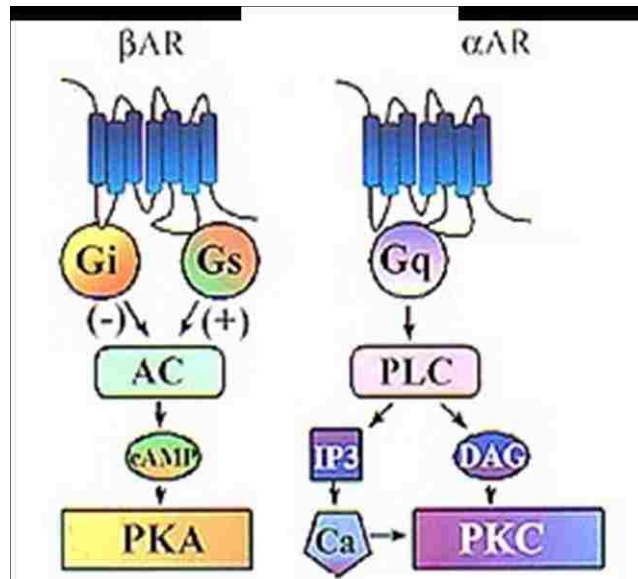


Figure 9. Norepinephrine Acts on its Target Cells by Binding to and Activating Alpha and Beta-Adrenergic Receptors (ARs).

The beta-adrenergic receptor (βAR) may couple either through Gi or Gs to adenylyclase in an inhibitory or stimulatory fashion, resulting in an increased formation of cyclic AMP and activation of protein kinase A (PKA). Activation of alpha adrenergic receptor results in activation of PLC. PLC cleaves phosphoinositol diphosphate (PIP2) into diacylglycerol (DAG) and inositol triphosphate (IP3). DAG activates PKC, with IP3 causing an increase in (Ca₂)i and other agonists, each through their own independent receptors, which can activate protein kinase C (PKC)⁵⁶.

1.5. Effect of Physical Cues on Differentiation

The physical cues that modify differentiation are defined by mechanical forces and discrete local architecture^{57, 58}. These conserved and evolutionary ancient features, although largely unknown, are the source of many signals. The signals are transduced to the cell nucleus through changes in cytoskeleton and complex signaling pathways. For example, it was shown that the fate decision of the oligodendrocyte precursors is controlled by both the spatial and geometric characteristics of an axonal niche. The critical cell density along an axon provides a mechanical stimulus promoting differentiation, possibly through alteration of the size or shape of the cells⁵⁹. Another example presented studies with mesenchymal stem cells (MSCs), where it was demonstrated that the size of the substrate pattern regulated cell shape, and cell shape through cytoskeletal tension, controlled the lineage commitment⁶⁰. The MSCs' fate has also been directed by the elasticity of the matrix resembling the specific tissue environment⁶¹. Hickman's group has previously demonstrated how physical as well as chemical cues control the function of endothelial and neuronal cells. In these studies, chemically defined surfaces and media were used to direct cell adhesion, proliferation, spreading and differentiation⁶²⁻⁶⁶.

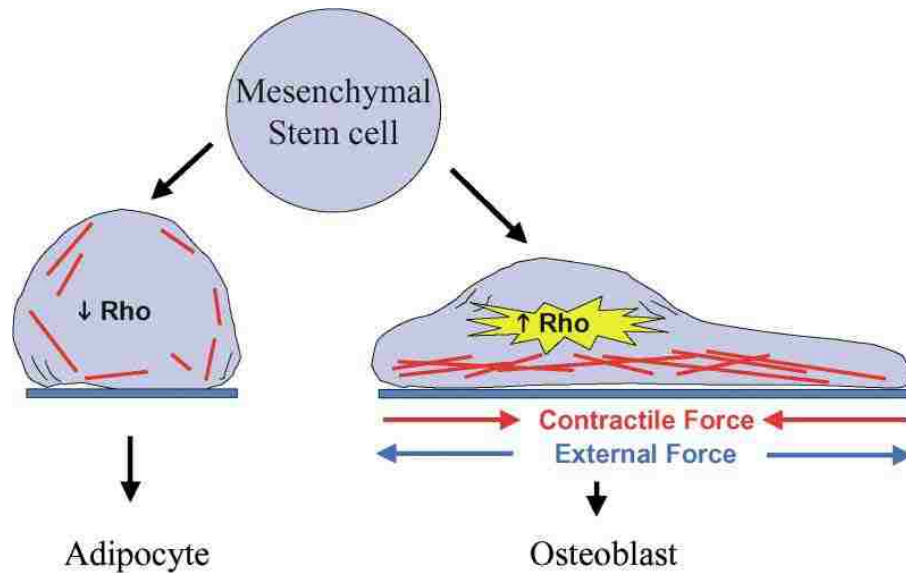


Figure 10. Schematic Illustration of the Role of Cell Shape and Cytoskeletal Tension in the Differentiation of MSCs.

When an uncommitted mesenchymal stem cell is plated on either a small (left) or large (right) island of fibronectin (blue lines), the consequent effect on cell shape, Rho GTPase activity, and cytoskeletal tension regulates the commitment to either the adipogenic or osteogenic lineage⁶⁷.

1.6. Differentiation of Human MLPCs from Umbilical Cord into Glia

In this study it was investigated whether the control of environmental conditions could induce differentiation of human adult stem cells into glia. Adult stem cells were utilized because they provide many advantages over fetal or embryonic stem cells. Adult stem cells are relatively abundant and easy to isolate. Furthermore, they are less likely to be rejected and do not appear to cause tumors after transplantation. Finally, there are no ethical considerations in harvesting adult stem cells. The adult stem cells in this study were human umbilical cord stem cells (hMLPCs).

The first goal of the study was to determine the effect of soluble environmental factors on differentiation of umbilical cord stem cells into oligodendrocytes. The soluble factors were represented by a number of molecules involved in stem cell differentiation or oligodendrocyte development. The major target was NE, previously shown to be involved in both stem cell differentiation and oligodendrocyte development^{43, 46, 48, 68}. NE is known to activate α and β adrenergic receptors expressed by its target cells, resulting in activation of associated downstream signaling pathways. The soluble factors alone in the standard 2D conditions were able to induce differentiation of hMLPCs along the initial stages of oligodendrocyte lineage.

The next goal was to investigate the effect of surface chemistry and geometry on differentiation of hMLPCs into oligodendrocytes. Previously published studies indicated that surface chemistry and geometry influenced stem and progenitor cell differentiation. For example, MSCs on large fibronectin islands differentiated into osteoblasts, while MSCs on small islands differentiated into adipocytes⁶⁰. However, the effect of surface chemistry and geometry on the glial differentiation of adult stem cells was not known. In order to recreate the right *in vivo* environment, with biology and engineering interacting at multiple levels, a novel 3D environment was constructed which guided differentiation of hMLPCs from umbilical cord into oligodendrocytes. The 3D environment was constructed from two sandwiched coverslips. The limited space between coverslips provided a defined environment within which cells resided and differentiated as well as provided surface cues to the top and bottom of the cells. All parameters were known and controllable. In the 3D environment, hMLPCs developed into oligodendrocytes and expressed the mature oligodendrocyte marker MBP. To facilitate oligodendrocyte functional assembly and to promote myelination *in vitro*, hMLPCs were co-cultured with rat embryonic

hippocampal neurons (EHNs). To examine whether the structural dimensions of the axon and the expression of membrane-bound axonal signals could provide sufficient physical cues for differentiation, the co-culture was performed in 2D and 3D culture conditions. The results indicated that after growth factor removal, hMLPCs developed into terminally differentiated oligodendrocytes in both 2D and 3D and wrapped their processes around the axons. To date, oligodendrocytes have been produced mostly from embryonic or fetal stem cells by other researchers. Differentiation of hMLPCs *in vitro* could generate an unlimited numbers of oligodendrocytes for studies of various differentiation stages or for transplantation to treat demyelinating diseases.

Finally, similar methodology was examined to determine if astrocytes could be differentiated from hMLPCs. It is known that oligodendrocytes and type 2 astrocytes develop from a common bi-potential progenitor^{28, 30, 69}. Astrocytes have been generated mostly from neural or embryonic stem cells by activation of several sets of ligands and receptors. For example, it has been shown that bone morphogenetic factors (BMPs) increase the percentage of astrocytes from neural stem cells while decreasing the production of neurons and oligodendrocytes^{70, 71}. Differentiation to astrocyte fate has been also accomplished by increased activity of leukemia inhibitory factor (LIF), basic FGF (bFGF), Notch signaling or with ciliary neurotrophic factor (CNTF)^{70, 72-81}. It has been demonstrated that CNTF caused transient commitment of O2-A progenitors toward a type 2 astrocyte fate^{73, 82}. A stable astrocyte fate has been achieved only in the presence of extracellular matrix-associated molecules, confirming the significance of environmental cues during cell differentiation and fate commitment. However, there are no published studies using NE to differentiate stem cells into astrocytes. In this study, astrocyte fate was achieved only in

the presence of physical cues provided by rat embryonic hippocampal neurons. After the induction of hMLPCs differentiation by NE and by physical contact with neurons, human astrocytes were separated from rat neurons by a density gradient and cultured further as a pure human astrocyte population. These results enable human astrocytes generated from the umbilical stem cells to be readily obtained and it would overcome many ethical issues associated with the use of embryonic or fetal stem cells.

2. MATERIALS AND METHODS

2.1. Modification of Surfaces

Glass coverslips (18x18mm², VWR,) were cleaned using HCl/methanol (1:1), soaked in concentrated H₂SO₄ for 2 hrs and then rinsed in double deionized H₂O. Coverslips were then boiled in deionized water, dried with nitrogen and cured at 110 °C in an oven. The trimethoxysilylpropyldiethylenetriamine (DETA, United Chemical Technologies), tridecafluoro-1,1,2,2-tetrahydroctyl- 1-trichlorosilane (13F, Gelest) and poly(ethylene glycol) (PEG, Sigma Chemical Co., St. Louis, MO) monolayers were formed by the reaction of the cleaned surfaces with a 0.1% (v/v) mixture of the organosilane in toluene (Fisher T2904). The DETA coverslips were heated to just below the boiling point of toluene for 30 min, and then rinsed with toluene, reheated to just below the boiling temperature, and then oven dried. Surfaces were characterized by contact angle and X-ray photoelectron spectroscopy methods as described previously⁸³.

2.2 Patterns Preparation

DETA/13F or DETA/PEG SAMs patterns were utilized in order to determine interaction on single cell level. These patterns consist of a co-planar monolayer of non-permissive and permissive regions: 13 F or PEG are the non-permissive, cytophobic regions of the DETA/13F or DETA/PEG SAMs patterns, respectively, while DETA monolayer is the permissive, cytophilic region of the SAMs patterns in both cases. Different approaches have been undertaken in order

to prepare the 2 types of SAMs patterns: the DETA/13F SAMs patterns were made by first patterning the DETA monolayer followed by a 13F backfill, while the DETA/PEG SAMs patterns were made by patterning the PEG monolayer followed by a DETA backfill. The SAMs of DETA or PEG were patterned using a deep UV (193 nm) excimer laser (Lambda Physik) at a pulse power of about 200 mJ and a frequency of 10 Hz for 45 seconds through a quartz photomask (Bandwidth Foundry, Eveleigh, Australia). The photomasks used in the patterning process differed also, depending on the type of SAMs patterns prepared, DETA/13F or DETA/PEG, respectively: a “positive” photomask consisting of chromium patterns on a transparent, quartz background (DETA/13F SAMs patterns), and a “negative” photomask consisting of transparent patterns on chromium background (DETA/PEG SAMs patterns). The energy dosage (8-15 J/cm²) was sufficient to ablate the regions of the SAMs monolayer exposed to the UV light, and yield reactive hydroxyl groups. The irradiated surfaces (DETA-derivatized SAMs or PEG- derivatized SAMs) were subsequently rederivatized with 13F, or DETA, respectively. The rederivatization with 13F was done in an inert atmosphere by the reaction of the irradiated surfaces with a 0.1 % (v/v) solution of 13F (Gelest, SIT8174.0) in dry chloroform (Sigma Aldrich, cat# 439142) for 5 min. The rederivatization with DETA was done as described above, but at lower temperature, 60°C.

2.3. Contact Angle Measurements

Water contact angle measurements were measured with a Ramé-hart goniometer (Mountain Lakes, NJ). The contact angle of a static sessile drop (5µl) of water was measured three times and averaged.

2.4. X-Ray Photoelectron Spectroscopy

The XPS characterization of DETA and PEG-silane surfaces was done with a Thermo ESCALAB 220i-XL X-Ray photoelectron spectrometer equipped with an aluminium anode and a quartz monochromator. The surface charge compensation was achieved by using a low-energy electron flood gun. Survey scans were recorded in order to determine the relevant elements (pass energy of 50 eV, step size= 1 eV). High resolution spectra were recorded for Si 2p, C 1s, N 1s, and O 1s (pass energy of 20 eV, step size= 0.1 eV).

The spectrometer was calibrated against the reference binding energies of clean Cu, Ag and Au samples. In addition, the calibration of the binding energy (BE) scale was made by setting the C 1s BE of carbon in a hydrocarbon environment at 285 eV. N 1s and Si 2p peak deconvolution was performed with Avantage version 3.25 software, provided by Thermo Electron Corporation.

Water contact angle on DETA was 48 +/-2. Water contact angle on PEG was 37 +/-2.

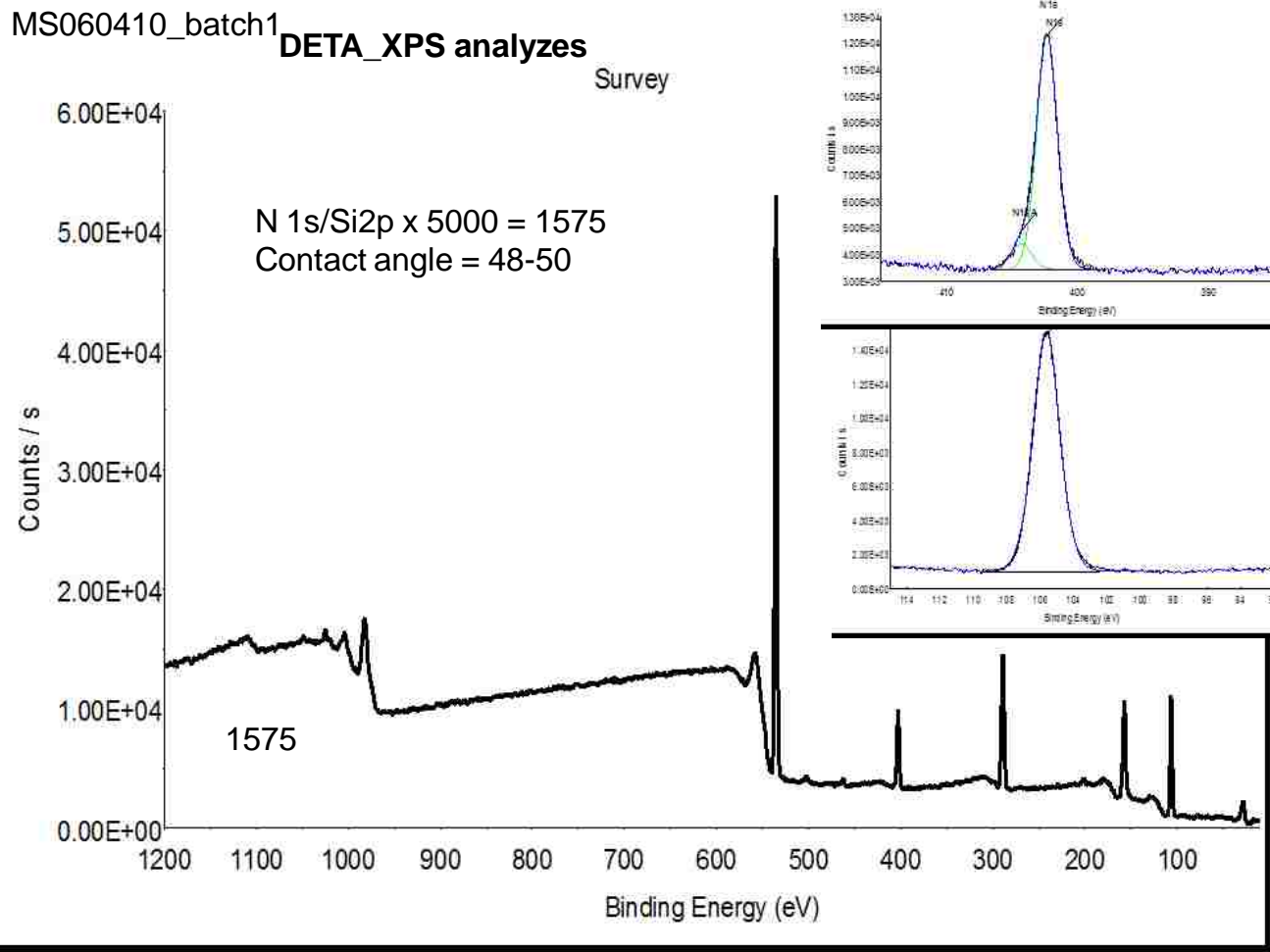


Figure 11. XPS Analysis of a DETA modified of Glass Coverslip.

2.5. hMLPCs Cell Culture

hMLPCs, human umbilical cord blood-derived clonal cell lines, passage 5, were purchased from BioE Inc., St. Paul, MN. The cells were cultured in tissue-culture treated T-75 flasks and maintained in growth medium, Dulbecco's Modified Eagle Media-high glucose (DMEM, Gibco BRL, Rockville, MD), with the addition of 15% fetal bovine serum (Stem Cell Technologies, Vancouver, BC) and 1% Antibiotic Antimycotic (Gibco BRL) at 37°C in humidified atmosphere containing 5% CO₂. The medium was changed every 3-4 days. Cells were passaged by trypsinization (0.05% trypsin/EDTA solution; Gibco BRL) upon reaching 60% confluence and replated at a 1:3 ratio. Passage 8 was used for the experiments unless otherwise indicated.

2.6. EHNs Cell Culture

All applied procedures were approved by the Institutional Animal Care and Use Committee of UCF. The protocol was modified from previously published work for embryonic rat hippocampal cultures^{65, 66, 84-86}. Pregnant rats, 18 days in gestation obtained from Charles River, were euthanized with carbon dioxide and the fetuses were collected in ice cold Hibernate E (BrainBits)/B27/GlutamaxTM/Antibiotic-Antimycotic (Invitrogen) (dissecting medium). Each fetus was decapitated and the whole brain was transferred to fresh ice cold dissection medium. After isolation, the hippocampi were collected in a fresh tube of dissection medium. Hippocampal neurons were obtained by triturating the tissue using a Pasteur pipette. In order to remove any debris from damaged cells the 1 ml cell suspension was layered over a 4 ml step

gradient (Optipep diluted 0.505: 0.495 (v/v) with the dissecting medium and then made to 15%, 20%, 25% and 35% (v/v) in the dissecting medium) followed by centrifugation for 15 min at 800 g and 4⁰C. After centrifugation, one strong band of cells was obtained. This band of cells was resuspended in culture medium (Neurobasal/B27/GlutamaxTM/Antibiotic-Antimycotic) and plated at a density of 100 cells/mm² on DETA coated coverslips or at a density of 75 cells/mm² on line pattern coverslips.

2.7. Induction of Oligodendrocyte Differentiation

hMLPC were seeded on DETA-coated glass coverslips (18 mm) at a density of 4x10³ cells/cm² in growth medium. After 3 days, at 60% confluence, the cells were incubated for 24 hours in pre-induction medium, consisting of DMEM, 15% FBS, bFGF, EGF (10 ng/ml each, R & D Systems, Minneapolis, MN) and PDGF-AA (10 ng/ml, Chemicon International, Temecula, CA). Pre-induction medium for neuronal differentiation was composed of DMEM, 15% FBS and bFGF (20 ng/ml). To initiate differentiation, the pre-induction medium was removed, the cells were washed 2x with Hanks' balanced salts solution (Gibco BRL) and transferred to serum free differentiation medium. Differentiation medium was composed of DMEM, N2 supplement (1%, Gibco BRL), 10 μM forskolin, 5 U/ml heparin (Sigma, St. Louis, MO), 5 nM K252a, bFGF, EGF, PDGF-AA (10 ng/ml each) and 20 μM NE (Sigma). The differentiation medium was changed every other day, while NE was added daily. For agonist experiments, norepinephrine was substituted with either the α1-adrenoceptor agonist isoproterenol or the β-receptor agonist isoproterenol (20 μM each, Sigma).

2.8. Co-cultures

EHNs were plated on DETA coated coverslips in hippocampal culture medium. After 4 days, half of the culture medium was replaced with serum free pre-induction medium consisting of DMEM, N2 supplement (1%, Gibco BRL), bFGF, EGF (10 ng/ml each, R & D Systems, Minneapolis, MN) and PDGF-AA (10 ng/ml, Chemicon International, Temecula, CA). After 24 hrs, another half of the medium was replaced with pre-induction medium and hMLPCs were plated on the top of the EHNs at cell density 5×10^3 cells/cm². After 24 hrs, half of the pre-induction medium was replaced with differentiation medium, composed of DMEM, N2 supplement (1%, Gibco BRL), 10 μ M forskolin, 5 U/ml heparin (Sigma, St. Louis, MO), 5 nM K252a, 20 μ M NE (Sigma), and with or without bFGF, EGF, PDGF-AA (10 ng/ml each). 24 hrs later, another half of the differentiation medium was replaced. After this medium replacement, half of the differentiation medium was changed every other day, while NE was added daily.

2.9. Construction of 3D Environment

hMLPCs were plated on DETA-coated glass coverslips (18 mm) in growth medium. At 60% confluence, growth medium was replaced with pre-induction medium. After the medium replacement, another set of coverslips was placed on the top of the cells. Prior to the placement, the top coverslips were ethanol sterilized and washed in the pre-induction medium. After 24 hours the pre-induction medium was removed, the cells were washed 2x with Hanks' Balanced

Salts Solution and transferred to serum free differentiation medium. The differentiation medium was changed every other day and NE was added daily.

2.10. Morphological Analysis

Phase-contrast images were taken with a commercial Nikon Coolpix 990 camera using the Zeiss Axiovert S100 microscope. Pictures were analyzed using Scion Image Software (Scion Corp., Frederick, MD).

2.11. Immunocytochemistry

To characterize cells by immunocytochemistry, the top coverslips, if present, were first carefully removed. Cells were then briefly washed with Hanks' balanced salts solution and fixed in 4% paraformaldehyde for 18 min. Fixed cells were stored in PBS, permeabilized with 0.5 % Triton 100x in PBS for 7 min, blocked with 5% donkey serum for 1 hr, followed by incubation with primary antibody overnight at 4°C. Primary antibodies were mouse monoclonal A2B5 (MAB312, 1:250), O4 (MAB345, 1:100), O1 (MAB344, 1:200), MBP (1:25), rabbit polyclonal anti-galactocerebroside (AB142, 1:200), Anti-Nuclei (HuNu), (MAB1281, 1:1000), Anti-Glial Fibrillary Acidic Protein (GFAP), (AB5804,1:2000), all from Chemicon, mouse monoclonal beta-2-AR (sc-81577, 1:200), rabbit polyclonal beta-1AR (sc-567, 1:250,) from Santa Cruz Biotechnology, alpha-1-AR (ab3462, 1:1000) and Neuron specific beta III Tubulin (ab18207, 1:250) both from Abcam Inc., Cambridge, MA. Following a PBS washing, cells were incubated with an Alexa Fluor 488-conjugated anti-mouse IgG or Alexa Fluor 488-conjugated anti-rabbit

IgG for 2 hours at room temperature. After a PBS washing, the coverslips were mounted with Vectashield mounting medium (H1000, Vector Laboratories, Burlingame, CA) onto slides. For general visualization of cellular nuclei, the specimens were counterstained with DAPI. Immunoreactivity was observed and analyzed by using an Ultra VIEW™LCI confocal imaging system (Perkin Elmer).

2.12 Isolation of Astrocytes by Discontinuous Percoll Gradients

For discontinuous Percoll gradients, 3 ml of 60% Percoll were added to the bottom of a 15-ml conical tube. Another 2 ml of 30% Percoll were slowly overlaid such that there was a sharp separation between the two concentrations. Without disturbing the gradient interfaces, the gradients were overlaid with 1 ml of the cell suspension. The gradients were transferred to a centrifuge and spun 10 min at $150 \times g$, at 4°C . The astrocyte-enriched fraction migrated to the buffer/30% Percoll interface, and the neuron-enriched fraction migrated to the 30%/60% interface. The astrocyte enriched layer was carefully aspirated. The cell suspension was transferred into a fresh 15-ml conical tube, containing 10 ml DMEM medium, high glucose, and centrifuged 10 min at $150 \times g$, at 4°C . Pelleted cells were resuspended in differentiation medium and plated on DETA coated coverslips.

2.13. Quantification

The morphological and immunocytochemical quantification was performed on undifferentiated stem cells or cells during various differentiation stages. For each coverslip, at least 10 pictures were taken from randomly chosen views under 200x magnification. All the marker-positive cells were counted, as well as the total number of cells in these views. At least three coverslips in each group were quantified and data were expressed as average \pm standard deviation (SD). Statistical differences between different experimental groups were analyzed by Student's *t*-test.

3. RESULTS

3.1 Acquisition of Neuronal Morphology

Motoneurons and oligodendrocyte are sequentially generated from a ventral population of neuroepithelial stem cells during development of the CNS^{25, 87}. Previous studies demonstrated involvement of NE in the differentiation of oligodendrocytes from oligodendrocyte precursors^{37, 48}. Other findings illustrated the influence of NE on development of spinal motoneurons and functional maturation of spinal cord⁴³⁻⁴⁵. However, the effect of NE on the generation of oligodendrocytes or motoneurons from stem cells is not known. Therefore, the influence of NE on differentiation of hMLPCs into motoneurons was investigated. Differentiation of stem cells along motoneuron or oligodendrocyte lineage is controlled by distinct molecular mechanisms influenced by various factors such as PDGF-AA, bFGF, EGF and changes in intracellular cAMP levels. These factors along with NE were employed to differentiate hMLPCs in a defined, serum free culture system. First, hMLPCs were plated on trimethoxy-silylpropyl-diethylenetriamine (DETA)-coated coverslips and allowed to evenly spread and expanded either for 3 days or to 60% confluence. At 60% confluence, the culture medium was replaced with the pre-induction medium supplemented with bFGF. After 24 hrs, cells were transferred into the differentiation medium. Differentiation medium contained the growth factors bFGF, EGF and PDGF-AA along with K252a, heparin, forskolin and NE. To determine the optimal dosage of NE, hMLPCs were treated with different NE concentrations, ranging from 10-500 μ M. Cells treated with 100-500 μ M concentrations of NE exhibited radical morphological changes within the first 4 hrs. Cell

bodies become smaller and round with the long process like extensions, resembling the morphology of neurons (Figure 12). However, in the continuous presence of NE, cells did not survive past 72 hrs. Thus, after 4hrs, once cells assumed neuronal morphology, differentiation medium was replaced with one deficient in NE. Once in differentiation medium lacking NE, cells retained their neuron like morphology for 72 hrs.

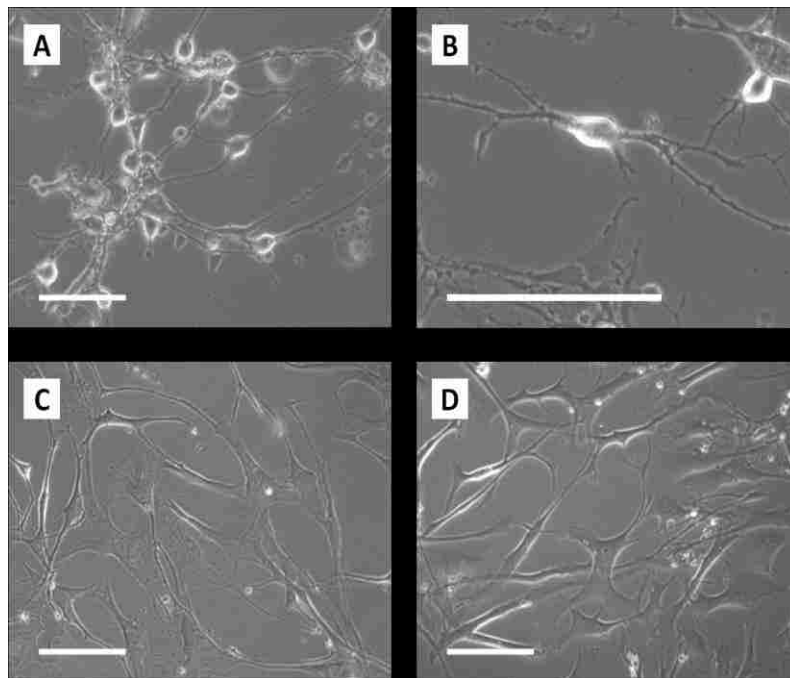
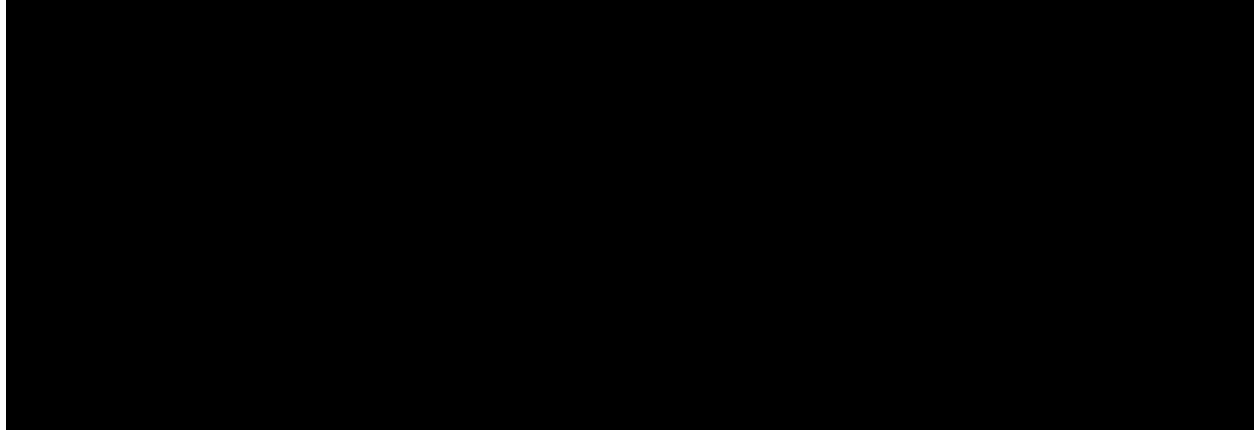


Figure 12. Phase Images of hMLPCs Treated with 100 μ M NE for 4 hrs.

(A) hMLPCs exhibit neuron like morphology at 4 hrs after treatment with 100 μ M NE. (B) Higher magnification image showing neuron like morphology of treated cells. (C) Untreated hMLPCs exhibit fibroblast morphology. (D) hMLPCs regained their fibroblast morphology 4 days after NE removal. Scale bars 100 μ m.

Table 1. Percentage of Cells Exhibiting Neuron-like Morphology in Response to NE.



3.2. Transient Expression of Neuronal Markers

In order to characterize these neuron like cells, immunocytochemical analysis was performed for expression of neuronal markers at 17, 36 and 72 hrs post induction (Figure 13). First, cells were stained for expression of nestin, known to be expressed by neural stem cells and progenitor cells. Results indicated that at 17 hrs post-induction $28.9 \pm 4.1\%$ of the cells expressed nestin. But after 36 hrs post induction all nestin expression was lost, suggesting the cells could progress to a more differentiated stage. Staining with neuronal marker β IIIIT revealed positive staining in $49.5 \pm 3.7\%$ of cells 17 hrs post induction and in $13.3 \pm 4.8\%$ of cells 36 hrs post induction. These cells also expressed motoneuron marker transcription factor Hb9, $87.2 \pm 12.5\%$ at 17 hrs and $94.2 \pm 3.3\%$ at 36 hrs post induction. However, 72 hrs after the treatment, the expression of neuronal markers diminished, the cells slowly flattened and regained their fibroblastic morphology.

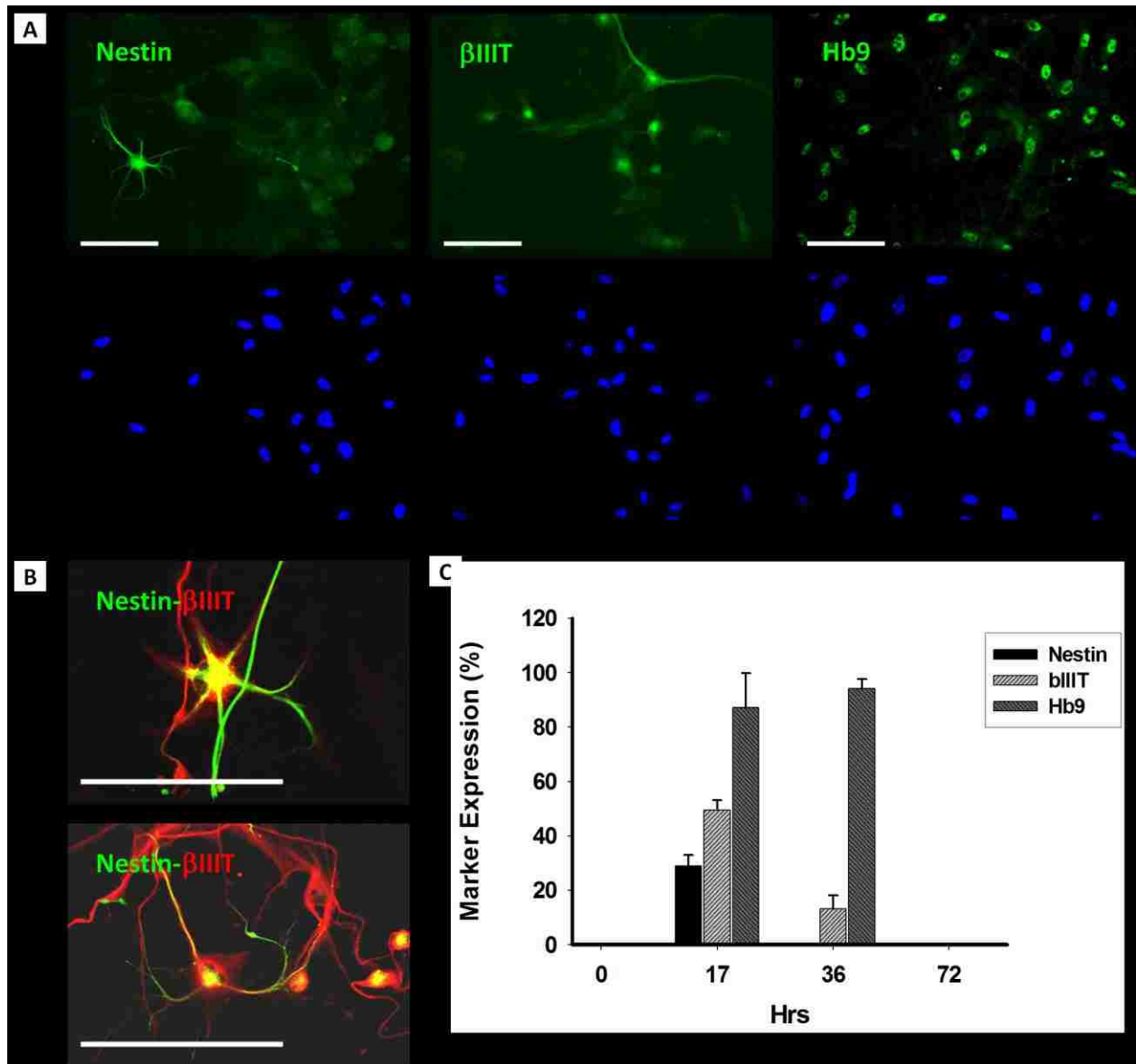


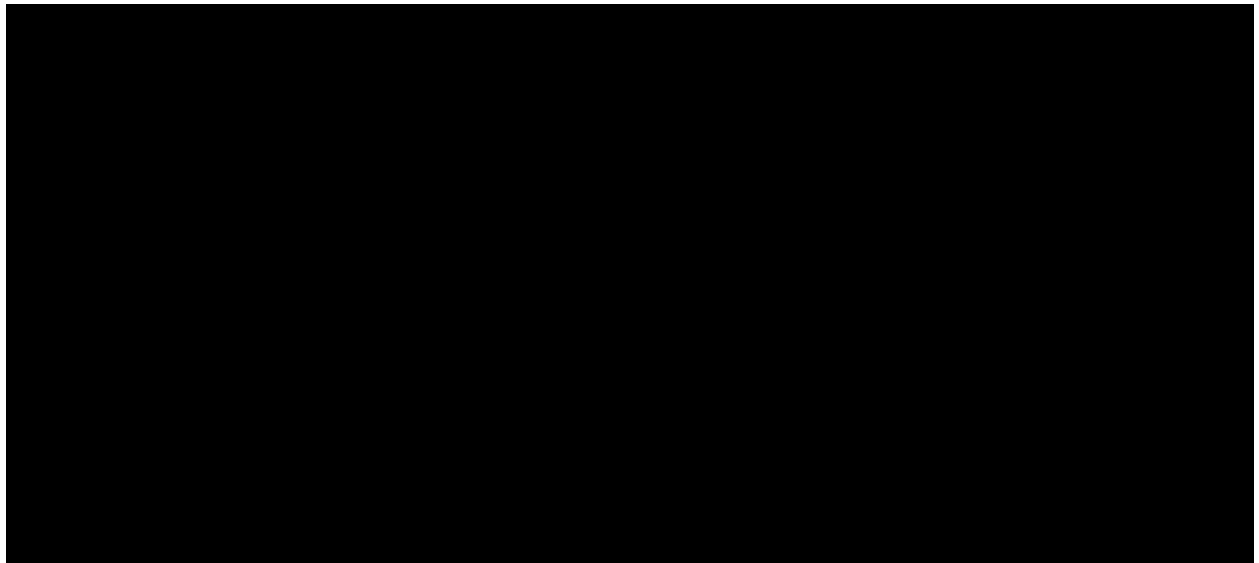
Figure 13. Transient Expression of Motoneuron Markers 17 hrs after Treatment with 100 μ M NE.

(A) hMLPCs transiently expressed nestin, β IIIT and Hb9 after the treatment. (B) Higher magnification images showing co-expression of nestin and β IIIT. All scale bars 100 μ m. (C)

Expression of neuronal markers 17 and 36 hrs after treatment. Error bars represent the SD.

To examine the effect of low dosages of NE on differentiation of hMLPCs, the cells were treated with 10, 20, 30 and 50 μM of NE daily (Table 2). Treatment with 10 μM NE did not induce any significant morphological changes within the first 2 weeks of treatment. Treatment with 30 μM resulted in increased cell death and treatment with 50 μM resulted in cell death within the first week. However, when cells were treated with 20 μM of NE daily, $67.1\pm 7.7\%$ of cells slowly contracted and developed multiple processes, resembling immature oligodendrocyte precursors, within 8 days of treatment.

Table 2. Percentage of Cells Exhibiting Oligodendroglial Morphology in Response to NE.



3.3. hMLPCs and Oligodendrocytes May Share Neuroepithelial Origin

Oligodendrocytes and motoneurons arise from the Sox1 positive neuroepithelium during development. Induction of oligodendrocyte fate is characterized by expression of A2B5 and PDGFR- α ^{30, 88}. In order to explore whether untreated hMLPCs could have some neuroepithelial or oligodendrocyte progenitor characteristics, immunocytochemical analysis for expression of Sox1, A2B5 and PDGFR- α was performed. The results indicated that untreated hMLPCs were Sox1 positive. This suggested that hMLPCs, like oligodendrocytes, originate from the neuroepithelium. Untreated cells were PDGFR- α positive and A2B5 negative but expressed PDGFR- β (Figure 14). The negative expression of A2B5 and positive staining for PDGFR- β distinguished the untreated hMLPCs from oligodendrocyte progenitor cells. These results are interesting when compared to recently published findings demonstrating that Sox1+ neuroepithelium also gives rise to the first wave of multipotent MSCs, generated during prenatal development^{89, 90}.

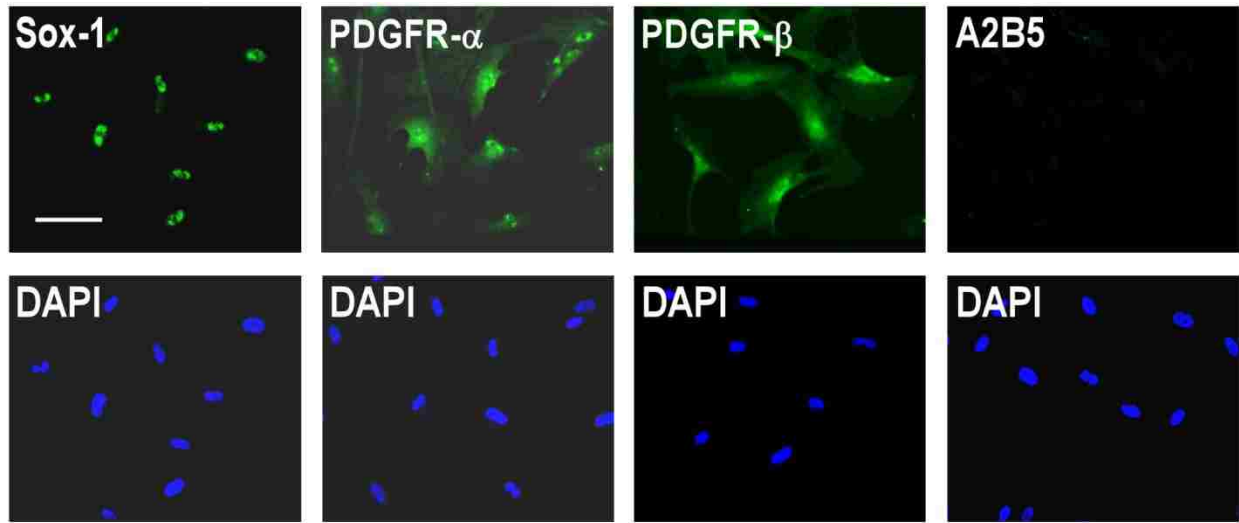


Figure 14. Immunocytochemical Analysis of Untreated hMLPC Suggest Neuroepithelial Origin.

Untreated hMLPCs expressed the neuroepithelial marker Sox-1, stained positively for PDGFR- α , PDGFR- β and negatively for A2B5. Scale bar, 100 μ m, (20x magnification).

3.4. Differentiation of hMLPCs in a 2D Environment

The development to an oligodendrocyte phenotype is influenced by factors such as PDGF-AA, bFGF, EGF and changes in intracellular cAMP levels. Based on these mechanisms, hMLPCs were induced to differentiate into the initial stages of the oligodendrocyte lineage in a defined, serum free culture system. Prior to differentiation, the hMLPCs were plated on DETA-coated coverslips and allowed to evenly spread and expanded either for 3 days or to 60% confluence. It was observed that higher cell densities reduced the differentiation efficiency, whereas low cell density negatively affected the survival. When the cells were 60% confluent, the culture medium was replaced with the pre-induction medium supplemented with bFGF, EGF and PDGF-AA. After 24 hrs, cells were transferred into the differentiation medium. Differentiation medium contained the growth factors bFGF, EGF and PDGF-AA along with K252a, heparin, forskolin and NE. The essential differentiation factors were NE, forskolin and K252a, as the desired morphology was not observed in the absence of any of these factors (Figures 15B, 15C, 15D). Both forskolin and K252a are factors frequently used during different stages of stem cell differentiation; however norepinephrine emerged as the novel stem cell differentiation factor that uniquely promoted the hMLPCs along an oligodendrocyte lineage. Absence of the growth factors increased the differentiation rate but resulted in decreased survival and less elaborate process formation (Figure 15E). After the transfer into the differentiation medium, the hMLPCs exhibited cell shape changes, from that of a fibroblast morphology (Figure 15A) to refractile cell bodies. Within 8 days of differentiation, approximately 70% of cells developed multiple processes and Figures 15F, 15G and 15H reflect the morphology development at day 15. During the process, a close correlation between the passage number and the differentiation potential was

observed. The most favorable outcome for differentiation of the hMLPCs was found when utilizing cells from passage 8. Earlier passages did not respond as well to the treatment and retained higher proliferation rates. Later passages exhibited a somewhat decreased differentiation capacity and a propensity towards senescence.

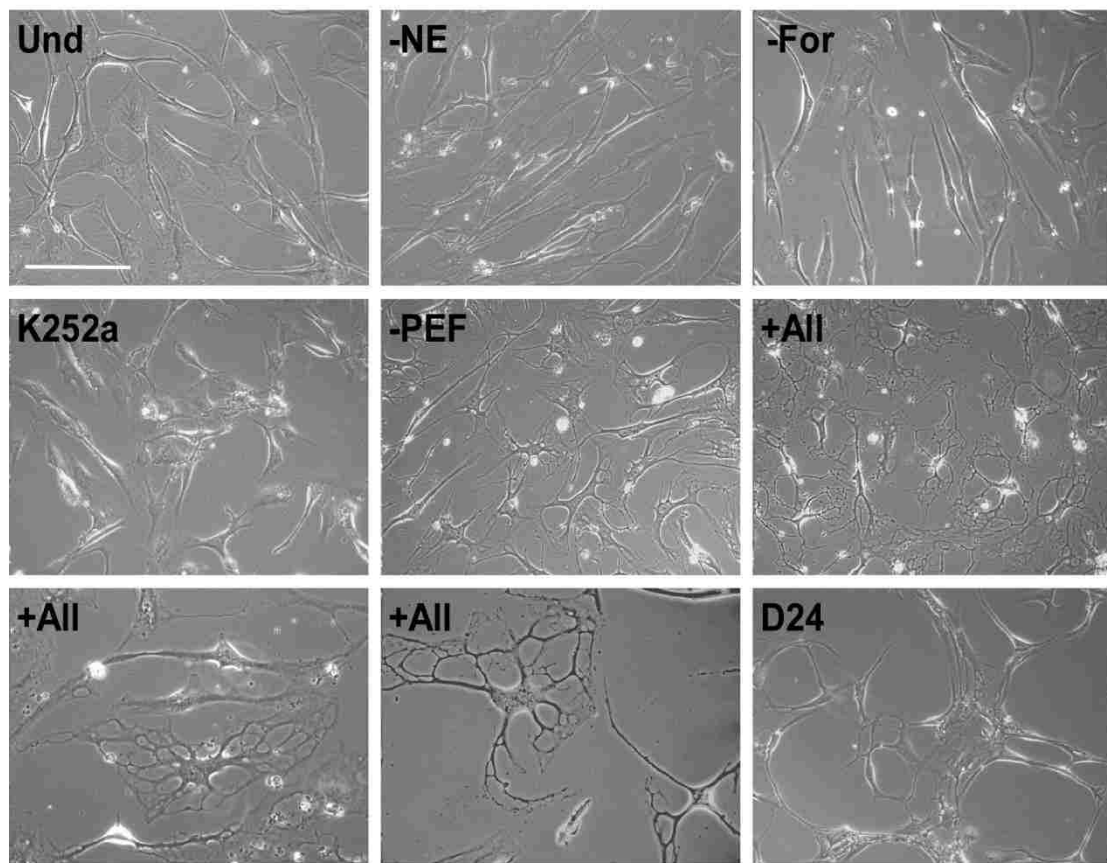


Figure 15. Phase Contrast Images of Differentiating hMLPCs in 2D Environment.

Undifferentiated (Und) hMLPCs exhibited fibroblast morphology. Cells at 15 days in differentiation medium without NE, forskolin (-For) or K252a retained their fibroblast morphology. Process formation was visible in the medium without growth factors (-PEF). Refractile cell bodies and increased process formation were observed in the presence of all factors indicated above (+All). Cells lost their multipolar morphology and became bipolar or spindle shaped at day 24. Scale bars, 100 μ m, (first two rows 20x magnification, third row 40x magnification (+All) and 20x magnification (D24)).

Immunocytochemical analysis was performed using the antibodies for specific stages of oligodendrocyte differentiation (Figures 16A, 16B). The untreated hMLPCs showed negative staining for A2B5 and faint staining for O4. Cells were also negative for the more mature oligodendrocyte markers O1 galactocerebroside and MBP. However, at 8 days of differentiation, $72.4 \pm 3.4\%$ of cells exhibited positive staining for A2B5 and $69.9 \pm 4.9\%$ for O4, but expression of O1 galactocerebroside and MBP was absent at this time period in the 2D environment. The results indicated that in response to the treatment, the majority of hMLPCs acquired cellular characteristics of immature oligodendrocyte precursor cells. The expression of A2B5 and O4, accompanied by a multi-process morphology, persisted to day 15, but the precursors did not achieve a fully differentiated oligodendrocyte phenotype. After 15 days of differentiation, cells began to lose their multi-process morphology and became mostly bipolar and spindle shaped (Figure 15I). At day 20, $35.0 \pm 4.8\%$ of cells remained A2B5 positive, $49.7 \pm 7.9\%$ O4 positive and O1, MBP negative (Figure 16B). In addition, limited cell survival was observed after day 20 in culture.

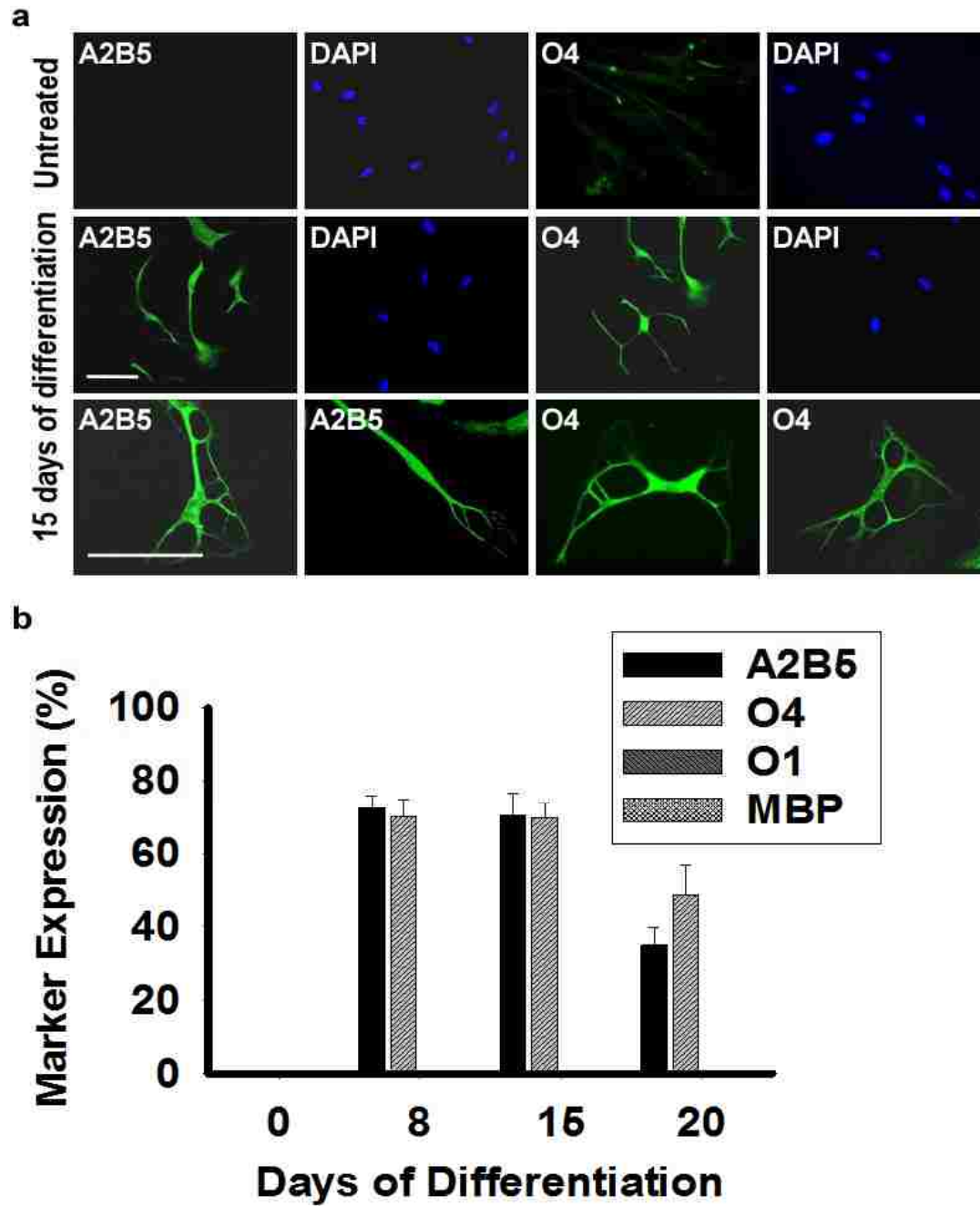


Figure 16. 2D Environment Promotes Differentiation of hMLPCs along Early Stages of Oligodendroglial Lineage.

(a) Immunocytochemical analysis of differentiating hMLPC in 2D environment. The untreated hMLPCs showed negative staining for A2B5 and faint staining for O4. At 15 days of differentiation, cells exhibited positive staining for A2B5 and O4, characteristics of immature oligodendrocyte precursor cells. (b) hMLPCs do not Differentiate into Committed Oligodendrocytes in a 2D Environment. At 8 days of differentiation, 72.4% of cells were positive for A2B5 and 69.9% for O4 and at day 15 70.3% of the hMLPCs exhibited positive staining for A2B5 and 69.7% for O4. At 20 days, 35.0% of cells remained A2B5 positive and 49.7% O4 positive. Expression of O1 galactocerebroside and MBP was absent in both untreated and differentiating cells. Scale bar, 100 μ m, (Rows 1 and 2, 20x magnification and Row 3, 40x magnification). Error bars represent the SD.

3.5. Differentiation of hMLPCs in a 3D Environment

Because it has been shown to be an important feature of cellular development, the effect of a simple 3D environment was examined on oligodendrocyte lineage progression. To construct this 3D environment, cells were differentiated between 2 coverslips. Initially, undifferentiated cells were plated onto DETA-coated coverslips at the bottom of 12-well plates. When the cells reached 60% confluence, the culture medium was replaced with the pre-induction medium, then, after the medium replacement, an unmodified glass coverslip was placed over the top of the cultured cells. In the 3D environment, within 24 hrs significant cell morphological flattening and spreading was observed (Figure 17B). After 24 hrs, the pre-induction medium was replaced with differentiation medium and there was a further increase in cell flattening (Figure 17C) but within 10 days of differentiation cells began to form processes and the cell bodies slowly contracted. Process development and branching continued for 3 weeks. After 30 days of differentiation, approximately 85% of the cells had elaborated an extensive network of processes (Figures 17D, 17E, 17F). The presence of PDGF was required for process formation, as in its absence cells progressed through initial differentiation stages but lost their multi-process morphology after 2 weeks of differentiation. The presence of bFGF and EGF was not essential but resulted in increased branching and the development of highly elaborated processes (Figures 17G, 17H, 17I).

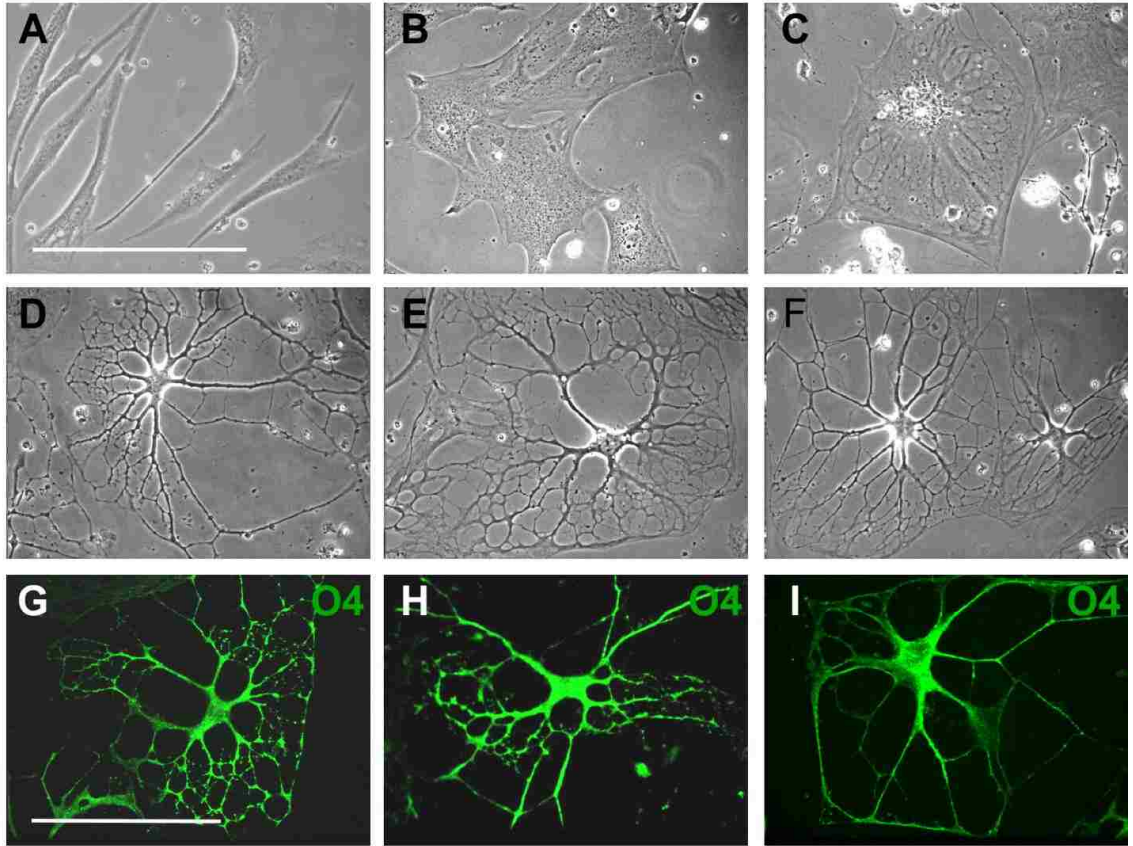


Figure 17. 3D Environment Promotes Further Differentiation of hMLPCs.

(A-F) Phase contrast images of differentiating hMLPCs. (A) The untreated cells displayed typical fibroblast morphology. (B) Cells exhibited flattening and spreading at 24 hrs in 3D environment. (C) Cells at 8 days in the differentiation medium displayed increased flattening. (D, E, F) At 30 days of differentiation, approximately 80% of cells revealed extensive processes. (G-I) Growth factors influenced the development of processes. (G, H) Immunostained cells displaying increased branching and development of processes in presence of bFGF and EGF. (I) Simple processes were observed in absence bFGF and EGF. Scale bars, 100 μ m, (40x magnification).

Immunocytochemical analysis revealed that after 20 days of differentiation $81.8 \pm 6.6\%$ of the cells expressed the oligodendroglial marker A2B5 and $80.6 \pm 2.9\%$ O4 (Figure 18C). At 30 days of differentiation, $57.7 \pm 3.6\%$ of the cells stained positively for A2B5, $79.6 \pm 2.9\%$ for O4, $42.1 \pm 2.7\%$ for the committed oligodendrocyte marker O1 galactocerebroside and $15.2 \pm 0.5\%$ for MBP (Figures 18A, 18B, 18C). The 3D environment appeared to play a key role during differentiation, oligodendrocyte commitment and lineage progression. There was decreased cell proliferation and, unlike in the 2D environment, passage numbers did not significantly affect differentiation in the 3D environment. Even after the removal of NE from the differentiation medium after 20 days, the cells retained their differentiated morphology for an additional 10 days in culture.

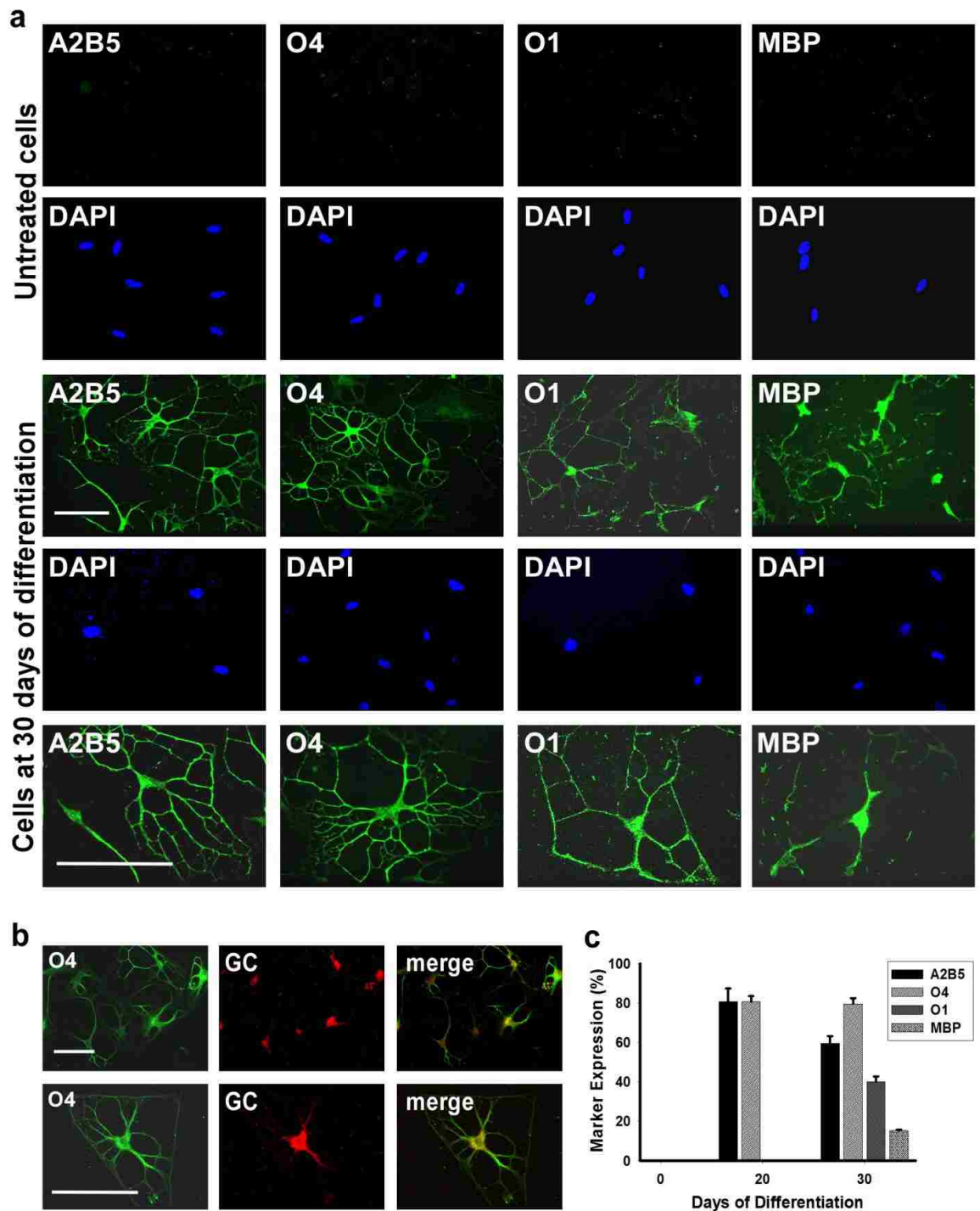


Figure 18. hMLPCs Differentiate into Committed Oligodendrocytes in a 3D Environment.

(A) Immunocytochemical analysis of differentiating hMLPCs in a 3D environment. The untreated hMLPCs indicated negative staining for A2B5, faint staining for O4 and negative staining for O1 galactocerebroside and MBP. At 30 days of differentiation, cells exhibited intensely positive staining for A2B5 and O4. Cells also expressed O1 galactocerebroside and MBP, characteristic of committed oligodendrocytes. Scale bars, 100 μm , (Rows 1-7, 200x magnification and Rows 4-5, 400x magnification). (B) Co-expression of O4 and galactocerebroside (GC) in the differentiated cells. At 30 days of differentiation, GC was expressed in O4 positive cells. Scale bars, 100 μm , (Row 1, 200x magnification and Row 2, 400x magnification). (C) The progression of differentiation in a 3D environment. At 20 days of differentiation 81.8% of cells expressed the oligodendroglial markers A2B5 and 80.6% O4 and were negative for O1 and MBP. At 30 days of differentiation, 57.7% of cells stained positively for A2B5, 79.6% for O4, 42.1% for committed oligodendrocyte marker O1 and 15.2% for MBP. Error bars represent the SD.

The contribution of the surface chemistry of the top coverslip was also qualitatively investigated as previously it has been shown that surface composition can have a dramatic effect on cellular response and differentiation^{63, 64, 91}. To determine the most appropriate 3D conditions for differentiation, the top glass coverslips were also modified with various surface chemistries which had been found previously to selectively promote or repel cell adhesion (Table 3). Unmodified glass coverslips were used as a control. To promote cell adhesion, the top coverslip was coated with a DETA monolayer. This environment, in which cells were attached to both top and bottom coverslips, produced initially good differentiation but eventually caused increased cell death, possibly due to damage from cell movement during feeding and morphological evaluation as the cells were well adhered to both surfaces. For the inverse situation the top coverslip was coated with polyethyleneglycol (PEG) or with a non-adhesive fluorinated silane (13F) monolayer. The PEG coated top coverslips resulted in good cell survival but a lesser degree of differentiation. 13F coated coverslips (contact angle >100°) triggered significant cell death. Thus it was determined that the glass coverslips controls were the most suitable top surfaces for optimal differentiation, as the cells did not adhere to the glass, and remained on the bottom DETA coated coverslips even after the top coverslip was removed.

Table 3. Percentage of Cells Developing Processes in Response to Surface Modification.

Development of processes (%)	Top Coverslip Modification			
	DETA	PEG	13F	Unmodified Glass
Day 20	66.9 ± 2.8	53.2 ± 1.3	38.1 ± 3.1	77.6 ± 2.2
Day 30	69.2 ± 10.4	55.5 ± 8.2	**	85.0 ± 2.1

Data show mean ± SD for three coverslips at day 20 and 30 of differentiation.

** No surviving cells were observed at day 30.

3.6. hMLPCs Express Functional ARs in the 3D System

To investigate the role of adrenergic signaling mechanisms in oligodendrocyte differentiation from the hMLPCs, immunocytochemical analysis was performed for expression of α - and β -ARs. The findings indicated that hMLPCs already expressed β 1-ARs on the cell surface before differentiation (Figure 19A). No expression of β 2-ARs before or during differentiation was detected. Expression of α 1-ARs was first observed at the nucleus and the intensity of staining significantly increased after treatment with pre-induction medium supplemented with bFGF, EGF and PDGF-AA (Figure 19B). Further analysis revealed that bFGF alone was able to increase nuclear expression of α 1-ARs (Figure 19C) in a time and dose dependent manner (results not shown). At day 15 of differentiation the α 1-ARs began to relocate to the cell surface. At day 30, differentiated cells expressed α 1-ARs at the surface of cell bodies and to a lesser degree in the processes (Figure 19B). This surface expression was observed only in cells with a multi-process morphology, whereas in cells exhibiting a flat morphology, or undifferentiated cells, the α 1-ARs remained at the nucleus. These studies are consistent with recent findings demonstrating nuclear localization of α 1-AR^{92, 93}. The published studies provided a new model for α 1-AR signaling, in which a signal is transduced from the nucleus to the plasma membrane, and is confirmed in this cellular transformation as well. The same initial expression patterns were noted in the 2D system, but the cells were not viable past day 20.

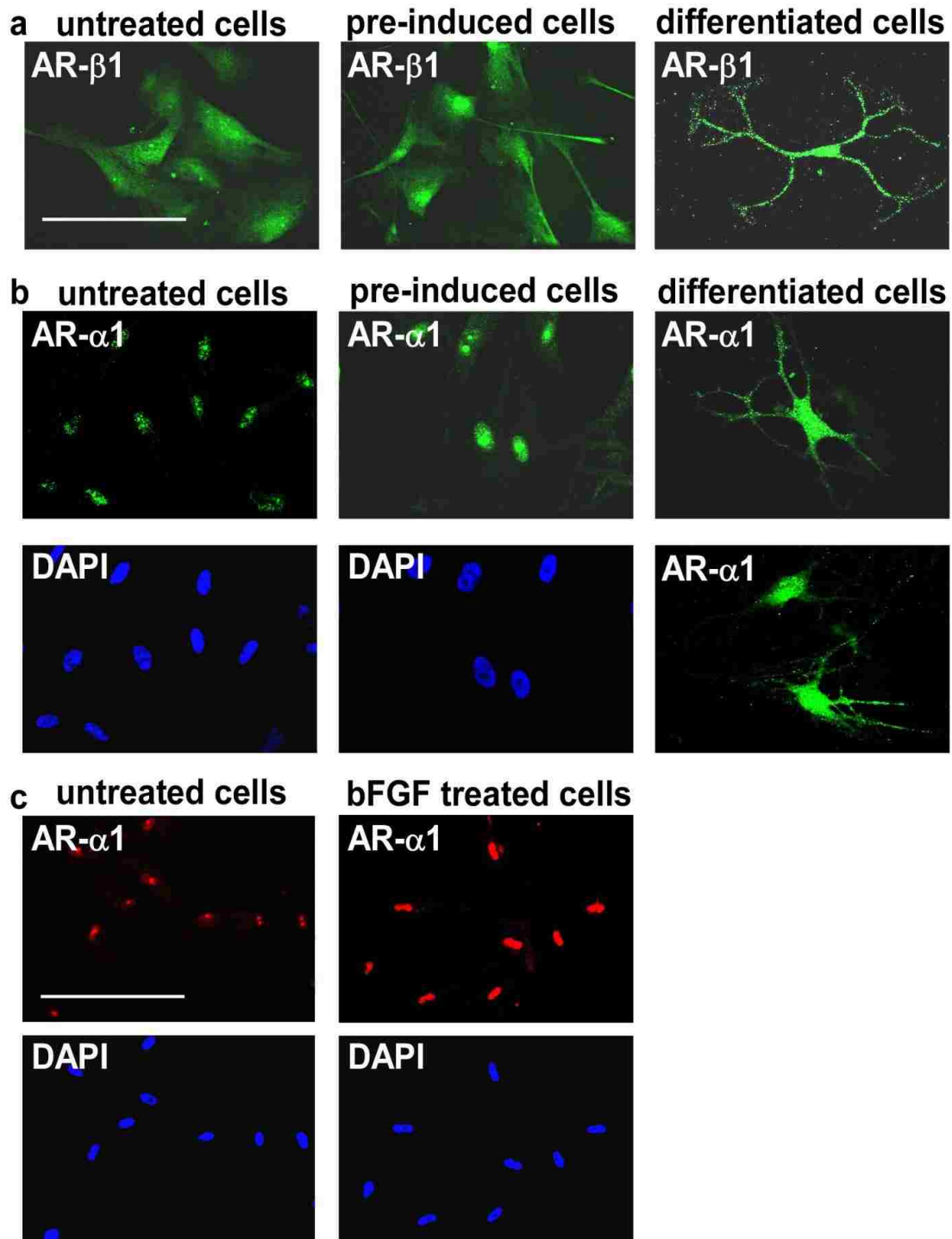


Figure 19. Expression of α 1- and β 1-ARs.

(a) Positive staining for β 1-ARs in undifferentiated cells, cells pre-induced for 24 hrs with bFGF, EGF and PDGF-AA, and cells at 30 days of differentiation. Scale bar, 100 μ m. (b) Nuclear expression of α 1-ARs in undifferentiated cells, intensive nuclear staining in cells pre-induced for 24 hrs with bFGF, EGF and PDGF-AA, and surface expression at 30 days of differentiation. (c) Nuclear expression of α 1-ARs in undifferentiated cells and evidence of a significant increase in staining intensity after 24 hrs treatment with bFGF alone. Scale bars, 100 μ m, (40x magnification).

3.7. Activation of Both α - and β -AR is Essential for Differentiation in the 3D System

To assess the role of each adrenergic receptor in the differentiation process, NE was substituted in the differentiation medium with equimolar concentrations of the β -AR agonist isoproterenol, the α 1-AR agonist phenylephrine or with both agonists. Daily treatment with isoproterenol induced morphological changes, cell body contraction and formation of processes within the first 15 days of treatment. However, approximately 60% of the cells displayed a bipolar morphology resembling immature oligodendrocyte progenitors. Cells did not change their bipolar morphology within 30 days of differentiation (Figure 20C) and exhibited enhanced cell death. In order to characterize these cells, immunocytochemical analysis at day 30 of differentiation was done. It was observed that $57.9 \pm 4.9\%$ of the cells expressed A2B5 and $42.5 \pm 2.7\%$ O4, however the cells were O1 and MBP negative (Figure 20G). These results demonstrated that stimulation of β -AR by isoproterenol induced the initial stages of differentiation. However, β -AR treatment alone was not sufficient to direct the MLP cells into a more mature stage of differentiation.

Daily treatment of the hMLPCs with the α 1-AR agonist phenylephrine initially resulted in only modest effects. Good cell survival was observed but the majority of cells maintained a flat morphology. Within 15 days of differentiation approximately 40% of the cells began to develop processes, however at day 30, only 15% of the cells exhibited more mature morphology with developed processes. The majority of cells showed only partial process development and branching or maintained a flat morphology (Figure 20D). Immunocytochemical analysis at day 30 revealed that $40.5 \pm 3.4\%$ of cells stained positively for A2B5, $39.8 \pm 2.8\%$ for O4 and $15.2 \pm 1.5\%$ for O1 (Figure 20G). The results suggested that activation of α 1-AR could play a role in

more advanced stages of differentiation in which cells start to lose expression of A2B5 and begin to express O1.

Daily treatments of cells with both isoproterenol and phenylephrine resulted in formation of multiple processes and the treated cells became morphologically similar to those treated with NE (Figures 20A and 20B). At day 30 of the differentiation period, $48.7 \pm 4.9\%$ of the cells stained positively for A2B5, $50.2 \pm 1.1\%$ for O4, $28.9 \pm 5.2\%$ for O1 and $9.7 \pm 0.7\%$ for MBP (Figures 20F, 20G).

The results indicate that stimulation of both the α - and β -ARs is required for optimal differentiation. This suggests a close interplay between both ARs, ultimately resulting in the expression of genes essential for oligodendrocyte development.

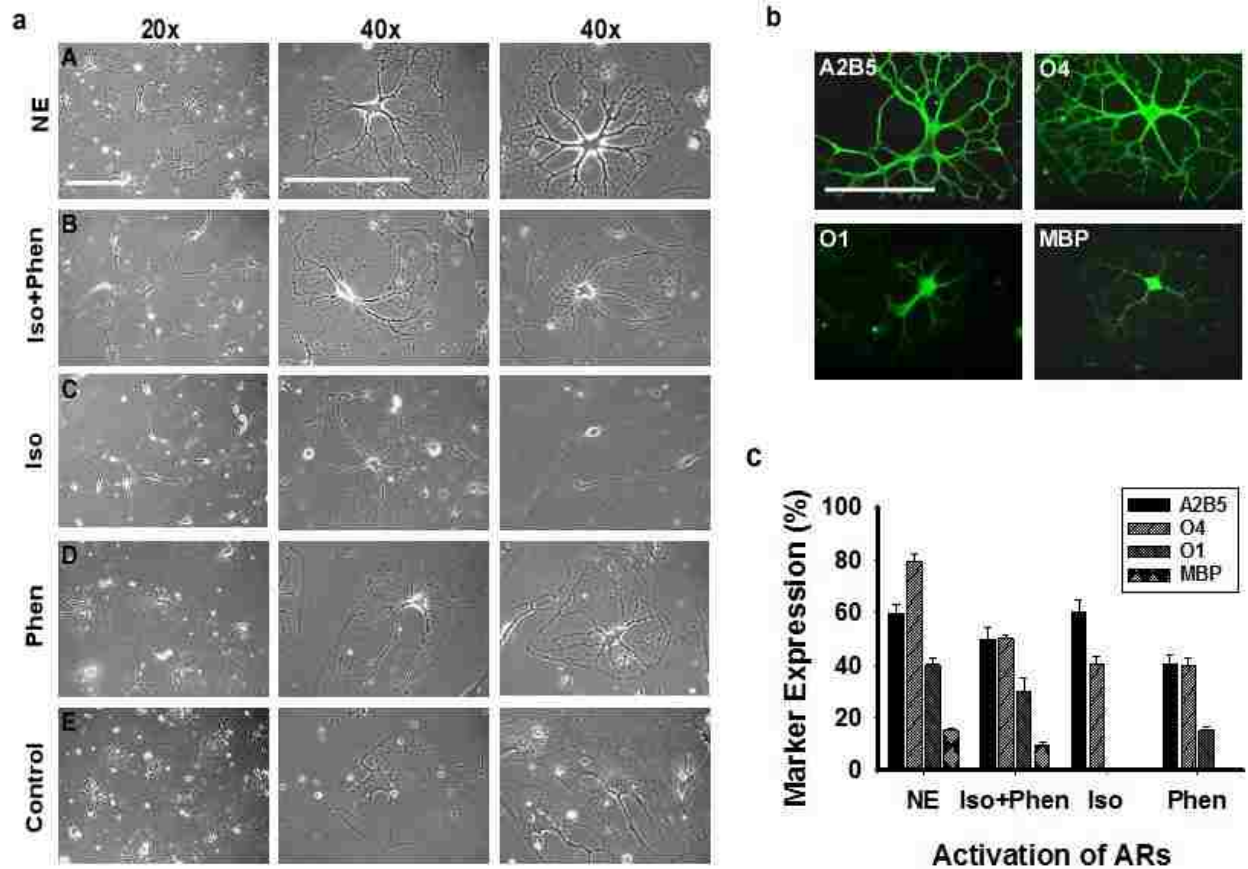


Figure 20. Influence of ARs on Differentiation of hMLPCs into Oligodendrocytes.

(a) Phase contrast images of cells at 30 days of differentiation, in the presence of NE, exhibited a complex multipolar morphology (A). Cells differentiated for 30 days in the medium where NE was substituted by the β -AR agonist isoproterenol and the α 1-AR agonist phenylephrine (B). Cells were morphologically comparable to cells treated with NE. Cells differentiated in the presence of the β -AR agonist isoproterenol frequently displayed bipolar morphology, resembling immature oligodendrocyte progenitors (C). Substitution of NE by the α 1-AR agonist phenylephrine resulted in mature morphology in 10% of the cells. The remainder of the cells showed only partial process development or remained flat (D). Cells differentiated for 30 days

without activation of ARs by NE or AR-agonists continued to exhibit a mostly flat morphology (E). (b) Stimulation of both α 1- and β 1-ARs is required for optimal differentiation. Immunocytochemical analysis of cells differentiated for 30 days in the presence of β -AR agonist isoproterenol and the α 1-AR agonist phenylephrine. Cells stained positively for A2B5, O4, O1 and MBP. Scale bars, 100 μ m. (c) Comparison of differentiation levels achieved by activation of both ARs by NE, by both AR agonists (Iso+Phen), by β -AR by isoproterenol (Iso) and by α 1-AR agonist phenylephrine (Phen). Error bars represent the SD.

3.8. Co-culture of hMLPC with EHNs

The engineered 3D culture environment provided essential physical cues to guide differentiation of hMLPCs into MBP positive oligodendrocytes. To facilitate their functional assembly and to promote myelination *in vitro*, hMLPCs were co-cultured with rat EHNs. It had been previously shown that differentiation of oligodendrocyte precursors is controlled by the spatial and geometric characteristics of an axonal niche⁵⁹. To examine whether the structural dimensions of the axon and the expression of membrane-bound axonal signals could provide sufficient physical cues for differentiation, the co-culture was performed in 2D and 3D culture conditions. To observe the interaction on single cell level, the cells were plated on DETA line patterns, separated by a cell repellent 13F coating. First, rat EHCs were plated on the coverslips containing the line patterns in hippocampal culture medium. After 4 days, half of the culture medium was replaced with serum free pre-induction medium. After 24 hrs, another half of the medium was replaced with pre-induction medium. 24 hrs later, hMLPCs were plated on the top of EHNs. 24 hrs later, half of the pre-induction medium was replaced with differentiation medium, composed of DMEM, N2 supplement, forskolin, heparin, K252a, NE and with or without growth factors: PDGF-AA, EGF and bFGF (PEF). 24 hrs later, another half of the differentiation medium was replaced. After this medium replacement, half of the differentiation medium was changed every other day, while NE was added daily. While the morphology of EHNs remained unchanged, significant changes were detected in morphology of the hMLPCs. Within first 48 hrs of co-culture, the cells contracted and developed rounded cell bodies with multiple processes (Figure 21). 3D cultures did not perform well as the cells adhered to both coverslips and it caused much cell death or were not noticeably different from the 2D conditions.

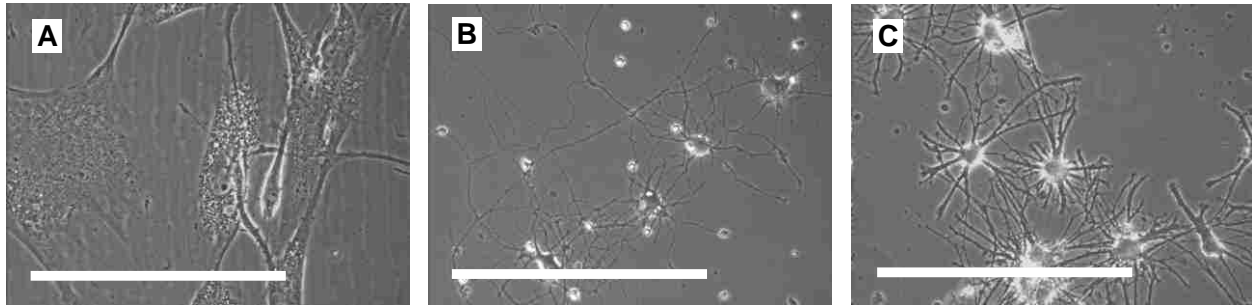


Figure 21. Morphological Changes of hMLPCs at 48 hrs after the Co-culture.

(A) Untreated hMLPCs before the co-culture exhibit fibroblast morphology. (B) Typical morphology of EHNs. (C) Rounded cell bodies and multiple processes of hMLPCs after the co-culture. Scale bars 100 μm .

As cells continued to differentiate, a morphological difference was observed related to the presence or absence of growth factors (PEF) in the medium. The difference in cellular morphology was markedly evident at 7 days of differentiation and became increasingly pronounced with increased differentiation time. Figure 18 reflects the cellular morphology at day 12. In the presence of growth factors in the medium, cells rapidly proliferated, spread, grew in size and developed long processes. Without the growth factors, cells remained smaller and in close contact with surrounding cells. A high proliferation rate was not observed, possibly due to a lack of growth factors and cellular contact inhibition. With increasing differentiation time, the distance between cells became shorter and after 3 weeks of co-culture, cells became so compact one could not clearly distinguish their morphology. These morphological changes were observed only in hMLPCs in physical contact with neurons. hMLPCs localized in the areas of low neuronal density, without physical contact with neurons, remained spindle shaped or flat. This suggests that physical cues provided only by axons were essential for differentiation in this system.

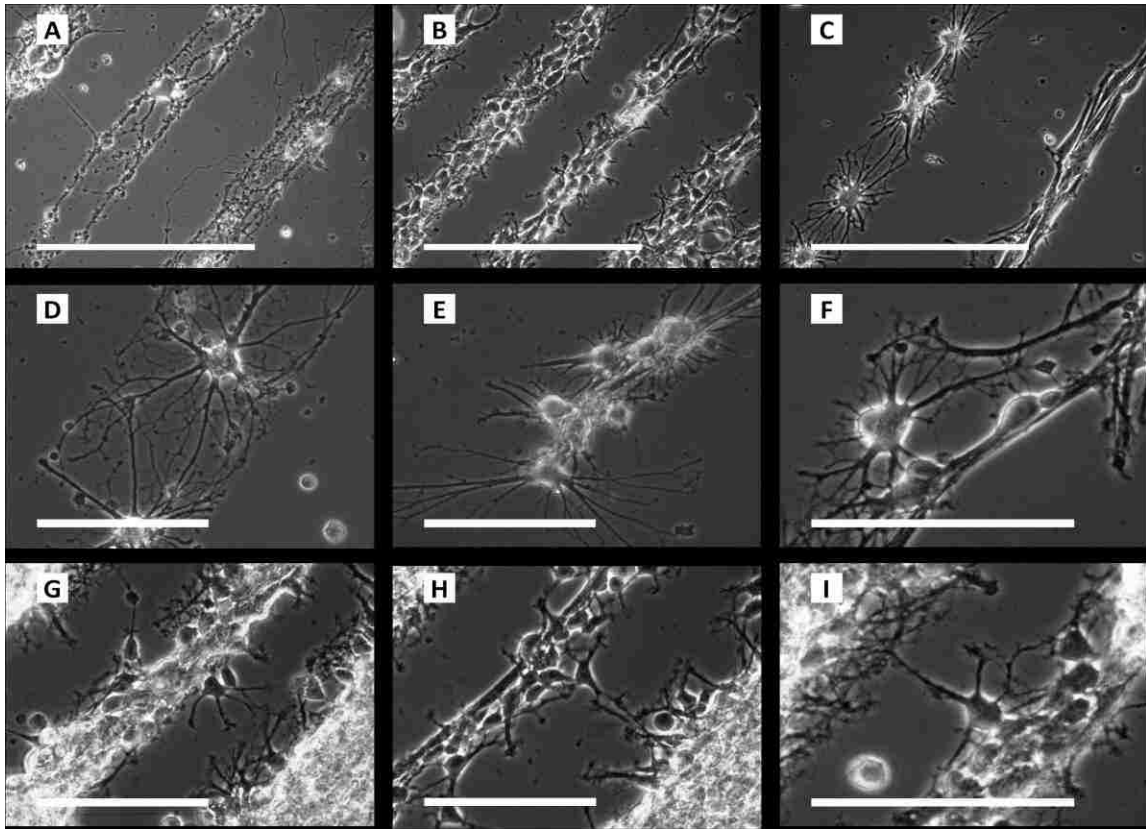


Figure 22. Phase Contrast Images of hMLPCs Co-cultured with EHNs.

(A) EHNs alone. Co-culture of hMLPCs and EHNs at 12 days of differentiation (B) in the absence of growth factors, (C) in the presence of growth factors. Higher magnification images of the co-culture differentiated (D-F) in the presence of growth factors and (G-I) in the absence of growth factors. Scale bars 100 μm .

3.9. Differentiating Human Oligodendrocytes can be distinguished from Rat Neurons

Differentiating hMLPCs were identified by immunocytochemistry using a monoclonal antibody against human specific nuclear antigen (HuNu). This antibody does not react with nuclei from rat. Rat EHNs were detected by employing neuron specific beta β IIIIT antibody. Untreated hMLPCs did not express neuronal β IIIIT, and HuNu immunostaining revealed their large nuclei. When hMLPCs were co-cultured with EHNs and induced to differentiate, approximately 70% cells significantly contracted and reduced in size. The same was true for changes of nuclear morphology. As cells continued to differentiate, their nuclei became rounded and substantially smaller. No significant changes were observed in the morphology of β IIIIT stained neurons. Immunocytochemical analysis of the co-culture at day 12 revealed that in presence of growth factors 66.8 ± 5.8 % of the cells stained positive for HuNu and 40.4 ± 5.5 % of the cells stained positive for β IIIIT. In absence of growth factors, 48.8 ± 3.1 % of the cells expressed HuNu and 55.6 ± 3.3 % expressed β IIIIT. The results of both conditions indicated that the human derived differentiating oligodendrocytes can be distinguished from rat neurons in this system.

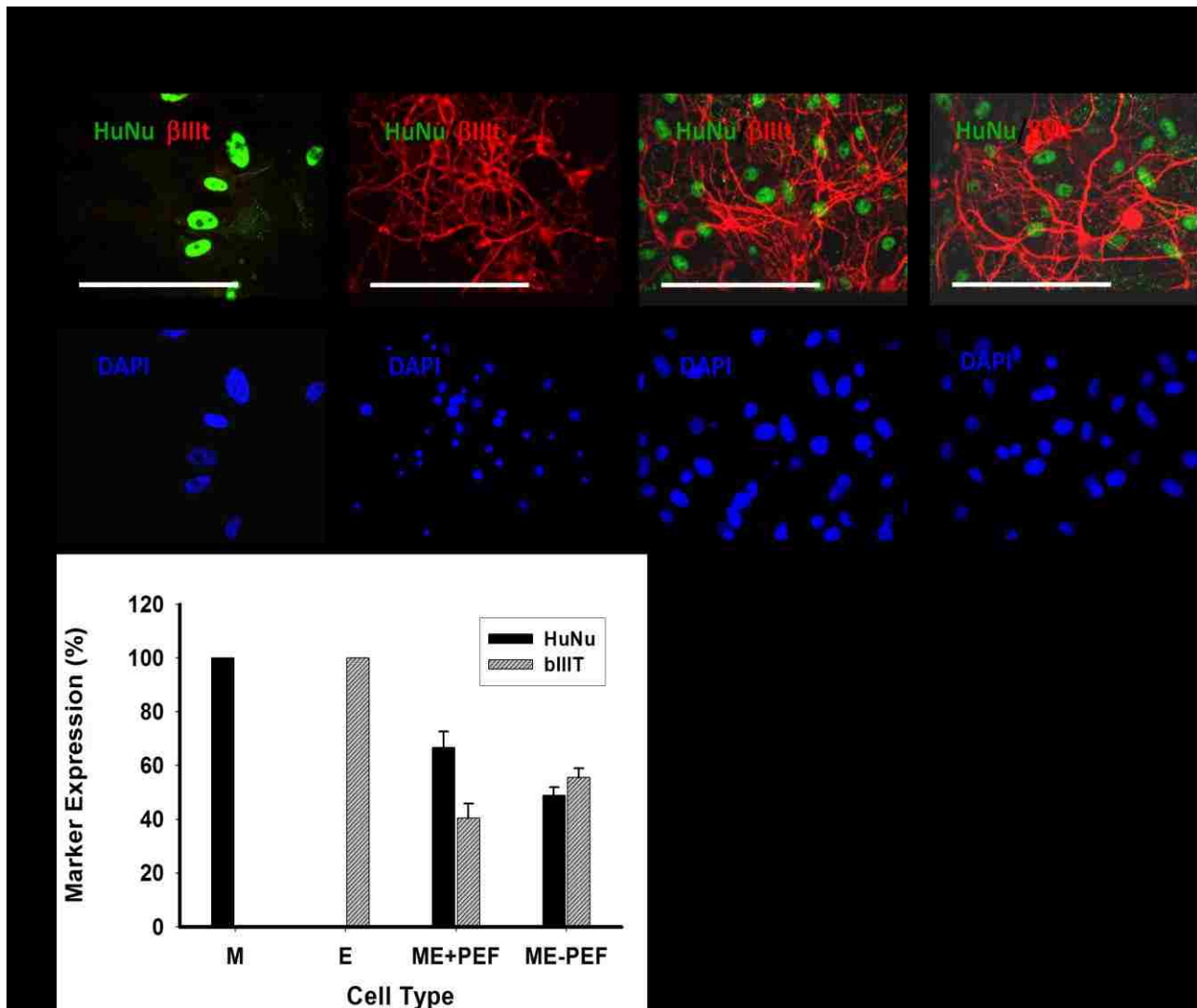


Figure 23. Immunocytochemical Analysis Distinguished hMLPCs from Rat EHNs.

(A) hMLPCs stained positively for human specific HuNu and negatively for β IIIIT. EHNs did not stain for HuNu but expressed the neuronal marker β IIIIT. The hMLPC and EHN co-culture at day 12 of differentiation showed positive staining for both HuNu and β IIIIT. Scale bars 100 μ m.

(B) hMLPCs alone stained 100% positively for HuNu and were negative for β IIIIT. EHNs alone stained 100% positively for β IIIIT but did not express HuNu. Co-culture at day 12 in the

differentiation medium containing PEF revealed that $66.8 \pm 5.8\%$ of the cells stained positively for HuNu and $40.4 \pm 5.5\%$ cells stained positively for β IIIIT. In absence of PEF, $48.8 \pm 3.1\%$ of the cells expressed HuNu and $55.6 \pm 3.3\%$ expressed β IIIIT. Error bars represent the SD.

3.10. hMLPCs Differentiate into Mature Oligodendrocytes in the Presence of EHNs

Differentiated cells were identified by immunocytochemical analysis for expression of oligodendroglial markers (Figure 24A). Results revealed that at 14 days of differentiation, in the presence of growth factors, $48.9\pm 6.2\%$ of the co-cultured hMLPCs expressed the bipotential oligodendrocyte/astrocyte progenitor marker A2B5 and $17.1\pm 3.4\%$ of cells expressed the early oligodendroglial marker O4 (Figures 24A and B). It was observed that the O4 positive cells were localized exclusively in the areas of highest cell density. Cells were negative for O1 and MBP. However, $39.3\pm 4.6\%$ of the co-cultured cells stained positively for the astrocyte marker glial fibrillary acidic protein (GFAP). These cells progressively exhibited long and sparsely branched processes, typical of type II astrocytes (Figure 24A). Some of the GFAP positive cells reached sizes up to $200\ \mu\text{m}$. These results suggested that in presence of growth factors, oligodendroglial differentiation of hMLPCs was arrested at the A2B5/O4 stage. It appeared that growth factors influenced the fate choice of proliferating bipotential A2B5 progenitors to become GFAP positive astrocytes. In absence of growth factors $44.2\pm 5.3\%$ of the cells stained positively for A2B5, $55.6\pm 3.3\%$ for O4, $20.2\pm 1.9\%$ for the committed oligodendrocyte marker O1 and $11.9\pm 4.2\%$ for MBP (Figures 24A and B). The O4, O1 and MBP positive cells were concentrated in the most cell dense regions. The results indicated that after growth factor removal, hMLPCs developed into terminally differentiated oligodendrocytes. These findings are consistent with previously published studies describing oligodendrocyte generation from A2B5 positive progenitors^{36, 94-96}. In these studies the progression from progenitor to myelinating oligodendrocyte entails a sequence of events, initiated by withdrawal of PDGF-AA and bFGF growth factors. This contributed to cell cycle withdrawal and cytoskeletal changes. In the

presence of neurons, terminally differentiated oligodendrocytes then wrapped their processes around the axons to initiate myelination.

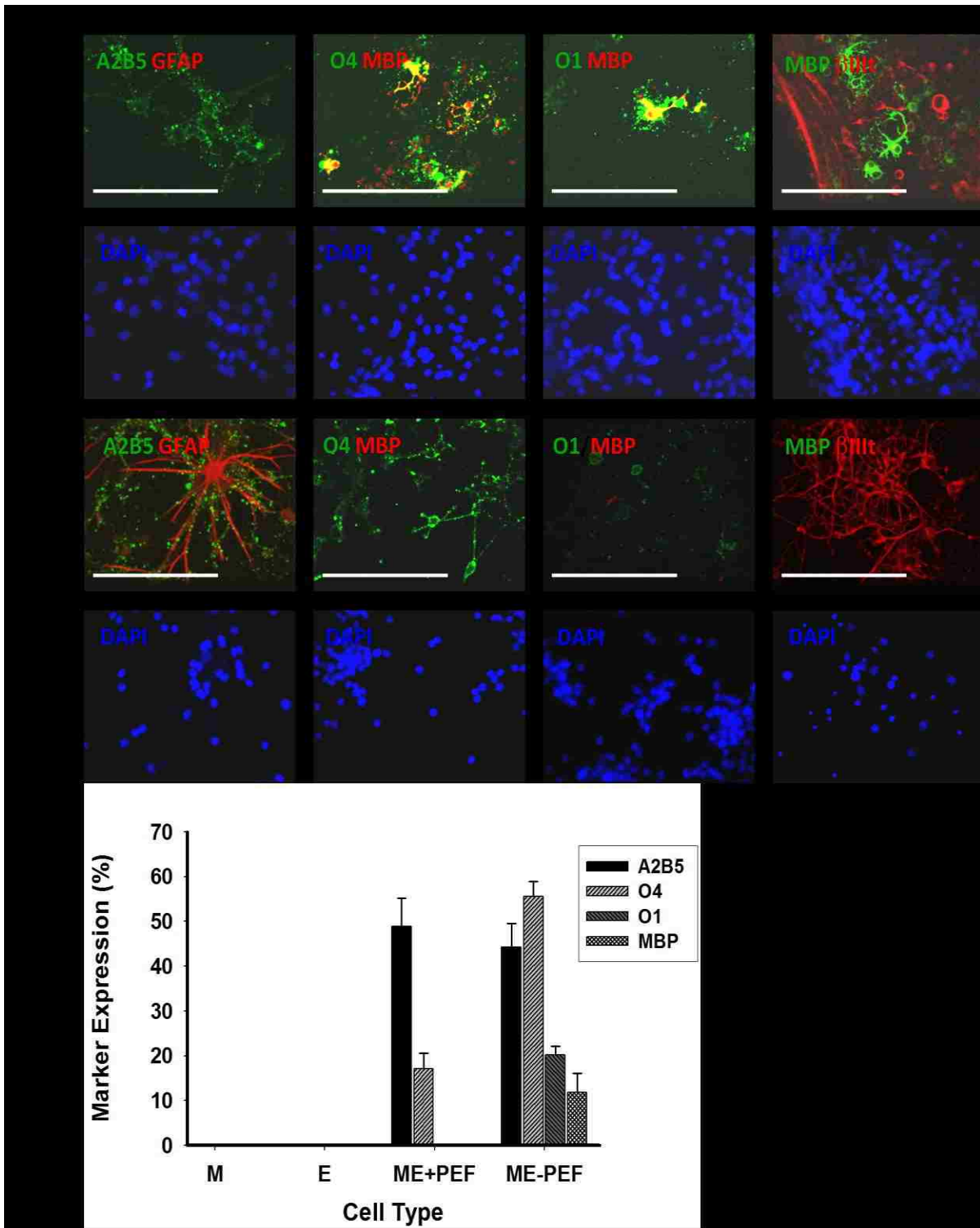


Figure 24. Immunocytochemical Analysis of Co-cultures Differentiated for 14 Days.

(A) In the absence of PEF, differentiated hMLPCs expressed the early and late oligodendrocyte markers A2B5, O4, O1 and MBP. In the presence of PEF cells did not progress into mature oligodendrocytes. Scale bars 100 μ m. (B) In the presence of PEF, $48.9 \pm 6.2\%$ of the co-cultured cells expressed the bipotential glial progenitor marker A2B5 and $17.1 \pm 3.4\%$ the marker O4 and were negative for O1 and MBP. In absence of PEF, $44.2 \pm 5.3\%$ of the cells stained positively for A2B5, $55.6 \pm 3.3\%$ for O4, $20.2 \pm 1.9\%$ for the committed oligodendrocyte marker O1 and $11.9 \pm 4.2\%$ for MBP. Error bars represent the SD.

3.11. Differentiated Oligodendrocytes Wrap around Axons in Culture

The primary function of oligodendrocytes is to produce the myelin sheath, which insulates axons of the CNS and facilitates rapid saltatory conduction of action potentials. To investigate whether the newly differentiated oligodendrocytes were functional and capable to myelinate the axons of rat EHNs, co-cultures were examined at day 21 by immunocytochemical analysis. At day 21, in the differentiation medium without growth factors, MBP positive oligodendrocytes exhibited elaborate processes and acquired a typical stellate appearance. It was observed that numerous primary processes of these cells emerged from the cell body and divided to form secondary processes. Tertiary processes then established interconnections between primary and secondary ones. These interconnections tended to appear first close to the cell body and then expanded further (Figures 25C and D). In the areas with high axonal density, oligodendrocytes aligned their processes along the length of axons and wrapped them around axonal fibers, that were labeled with the neuronal marker β IIIIT (Figures 25A and B).

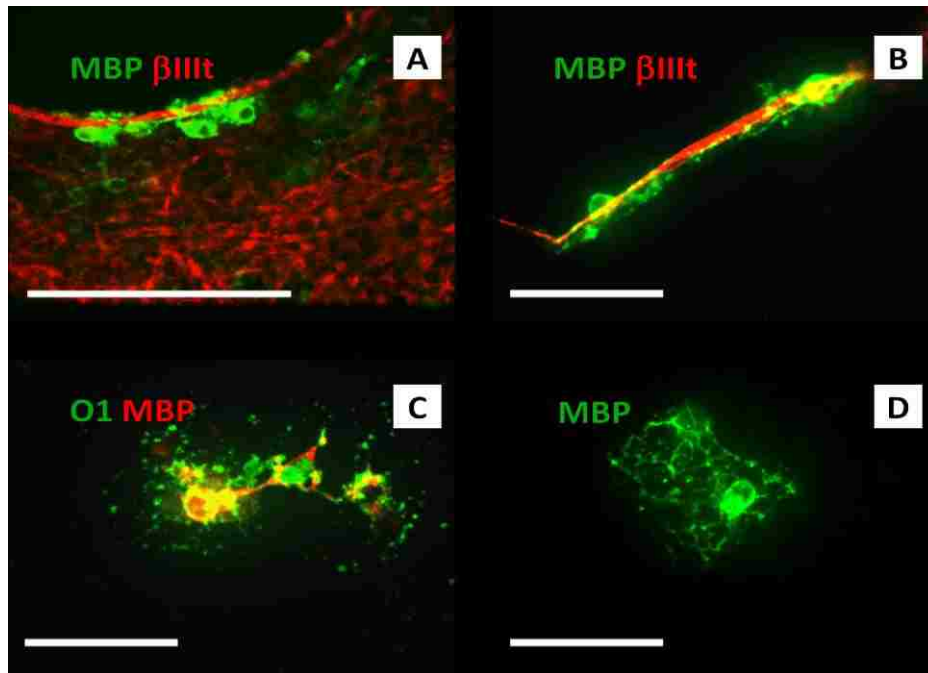


Figure 25. Immunocytochemical Analysis of Mature Oligodendrocytes.

(A) Oligodendrocytes wrapping their processes around axons. Scale bar 100 μm . (B) Mature oligodendrocytes wrapped around an axon. Scale bar 50 μm . (C-D) Morphology of mature oligodendrocytes. Scale bars 50 μm .

3.12 Generation of Pure Astrocyte Population

In order to generate a pure astrocyte population, differentiated astrocytes were separated from rat neurons using a density gradient. For this purpose, cells were trypsinized of the culture surface at day 5 of co-culture and passed through a Percoll gradient. The small neurons passed through the 30% Percoll and come to rest on a cushion of 60% Percoll. The larger, membranous astrocytes stopped at the medium/30% Percoll interface.

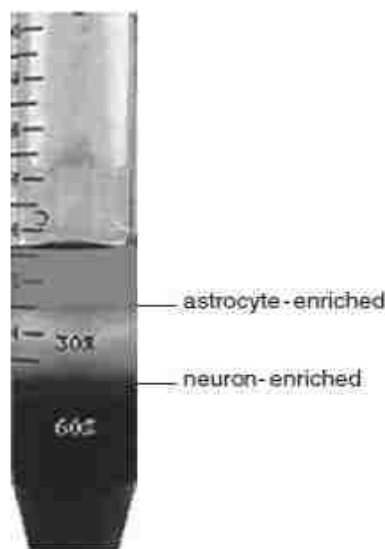


Figure 26. Percoll Gradient Separation of Astrocytes⁹⁷.

Isolated astrocytes were then replated on DETA coated coverslips and cultured further in the differentiation medium. After 5 days, immunocytochemical analysis was performed for the astrocyte markers GFAP and S100 and for the human specific markers HuNu and human microtubule marker.

The results indicated a pure human derived astrocyte population (Fig.27)

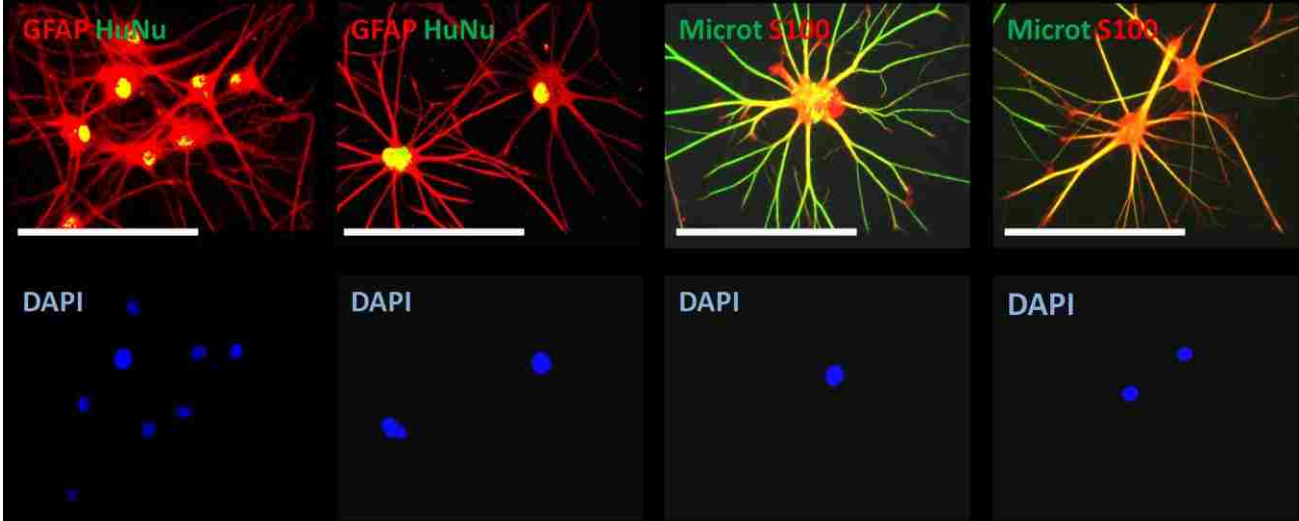


Figure 27. Immunocytochemistry of Astrocytes Isolated by Percoll Gradient.

4. DISCUSSION

Motoneurons, oligodendrocytes and astrocytes are produced during CNS development from a restricted domain of the ventral ventricular zone, termed the pMN domain⁹⁸. These cells sequentially arise from Sox-1 positive neuroepithelial cells of the neural tube¹⁶⁻¹⁸. In this study, functional oligodendrocytes were generated from Sox-1 positive hMLPCs from human umbilical cord. It is possible that hMLPCs, like cells of the CNS and early waves of multipotent MSCs, originate from neuroepithelium during development^{89, 90}. hMLPCs from umbilical cord are collected at birth and have the potential to give rise to all three embryonic layers⁹⁹. This study has indicated that hMLPCs display extreme sensitivity to their environment. Their fate depends not only on soluble factors but also on the surrounding physical cues. The combination of these external signals, processed through signal transduction networks, altered the cell morphology, induced transitional expression of motoneuron markers and finally, influenced fate decision to differentiate along the oligodendrocyte lineage. Various published findings have illustrated the influence for NE on development of spinal motoneurons and the functional maturation of spinal cord⁴³⁻⁴⁵. For example, it was illustrated that noradrenergic innervations of the ventral horn rapidly peaks during development of the spinal cord and then declines at the end of neonatal life to the values found in the young adult. The rapid increase of NE levels during prenatal development suggests a significant role for NE in the differentiation of motoneurons. In other studies, electron microscopy images have provided evidence for direct noradrenergic control of oligodendroglial and astroglial cells throughout the cortex⁴⁸. Oligodendrocytes were the major target of the noradrenergic fibers, exhibiting a light thickening at the sites of contact. It was

reported that oligodendrocytes expressed $\alpha 1$ and β -ARs and their activation by NE accelerated differentiation of the oligodendrocyte precursors^{37, 49, 51}. In spite of this, there were no known studies using NE as a key factor to induce differentiation of stem cells into oligodendrocytes. To explore this possibility, hMLPCs were analyzed for expression of ARs, and it was found that the undifferentiated cells expressed both $\alpha 1$ -ARs and $\beta 1$ -ARs. The $\beta 1$ -ARs were localized on the surface before and during the differentiation. Surprisingly, typical surface expression of the $\alpha 1$ -ARs was not observed; instead, the $\alpha 1$ -ARs were localized at the nucleus. The intensity of nuclear staining significantly increased after treatment with bFGF. However, as the cells exhibited a more differentiated phenotype after 15 days of differentiation and then relocation of $\alpha 1$ -ARs to the surface was observed. Nuclear localization of $\alpha 1$ -ARs is consistent with a recently proposed model for $\alpha 1$ -AR signaling in cardiac myocytes. In this new model, activation of $\alpha 1$ -AR signaling is initiated at the nuclear membrane and results in localization of activated ERK in calveolae at the plasma membrane^{92, 93}.

Differentiation was initiated by the transfer of hMLPCs into the differentiation medium in a 2D environment. The differentiation medium contained NE along with forskolin, K252a, heparin, PDGF-AA, bFGF and EGF. Within 8 days in the differentiation medium, process formation was observed and immunocytochemical analysis indicated a positive reactivity to A2B5 and O4 primary antibodies. In spite of this, cells did not progress further along the oligodendrocyte lineage. After 2 weeks in differentiation medium, cells exhibited bipolar and spindle like morphology and remained A2B5 and O4 positive, but O1 negative, and prolonged differentiation time also significantly increased cell death.

A 3D microenvironment was constructed to combine chemical and physical cues shown to influence lineage commitment during development in other systems. The hMLPCs responded to the 3D environment initially by cell flattening and later, within 2 weeks of differentiation, formation of processes. At 30 days, $42.1 \pm 2.7\%$ of cells expressed the O1 antigen, indicating terminally differentiated oligodendrocytes, and $15.2 \pm 0.5\%$ of the cells expressed MBP with increased cell survival. The differentiated cells survived for more than 40 days in culture. Importantly, the oligodendrocytes retained their differentiated state even after removal of the NE after 20 days.

It is well established in other systems that after removing growth factors from the medium, oligodendrocyte precursors exit cell cycle, stop dividing and terminally differentiate¹⁰⁰⁻¹⁰². In our system, more complex branching, process development and increased survival was demonstrated in the presence of growth factors. This could be explained by the combined effect of forskolin and norepinephrine. Both factors are known to increase cAMP levels, and increased cAMP levels inhibit proliferation of oligodendrocyte precursors^{37, 103}. Thus, the removal of growth factors was not essential for cell cycle exit and terminal differentiation. Decreased proliferation with increased cell flattening and spreading was also observed after the introduction of the top coverslip.

It has also been demonstrated previously that stimulation of β -ARs induces differentiation through an increase in intracellular cAMP and through the activation of proteins known to be involved in cell cycle arrest³⁷. There are also studies revealing that p38MAPK and Erk1/2 have roles in differentiation of oligodendrocyte progenitors¹⁰⁴. Both ARs can activate p38MAPK while Erk1/2 is a downstream target of α 1-AR. It was shown in these studies that p38MAPK

activity was required for the progression of bipolar early progenitors (A2B5+, O4-) to multipolar late progenitors (O4+, O1-), and Erk1/2 activity was essential for progression of late progenitors to oligodendrocytes³⁶.

Our results indicated that the majority of cells treated with the β -AR agonist isoproterenol remained bipolar even after 30 days of differentiation. Immunocytochemical analysis indicated differentiation arrest at the stage where A2B5+ cells began to express O4, perhaps due to insufficient activation of Erk1/2 signaling. In contrast, cells treated with the α 1-AR agonist phenylephrine showed higher survival and after 30 days of differentiation $15.2 \pm 1.5\%$ of cells had progressed to the O1+ stage, possibly due to increased stimulation of the Erk1/2 signaling pathway. However, simultaneous activation of both receptors by NE, or by both agonists, was the best strategy, possibly by supplying the optimal cAMP levels and stimulating essential signaling pathways engaged in the close interplay during differentiation. This study demonstrated the significance of cellular microenvironment as a driving force in human stem cell differentiation. A 3D environment was constructed and a novel small molecule was utilized to induce differentiation of hMLPCs, whereas neither condition alone produced functional differentiation. The mechanical cues in combination with soluble factors influenced the progression of hMLPCs along the oligodendrocyte lineage.

To investigate whether hMLPCs' derived human oligodendrocytes are functional and capable to myelinate axons, hMLPCs were co-cultured with rat EHNs. Because axons could also provide physical cues to influence functional differentiation, the co-culture was performed in 2D as well as 3D conditions. Our results indicated that structural dimensions of the axons and the expression of membrane-bound axonal signals provided sufficient physical cues for differentiation in 2D

conditions. In co-culture, hMLPCs differentiated into mature oligodendrocytes or astrocytes based on presence/absence of growth factors in differentiation medium. In the absence of PDGF-AA, EGF and bFGF, hMLPCs differentiated into oligodendrocytes.

At day 21, in the differentiation medium, MBP positive oligodendrocytes exhibited elaborate processes and acquired a typical stellate appearance. The formation of elaborate processes was observed and in the areas with high axonal density, oligodendrocytes aligned their processes along the length of axons and wrapped them around the rat axonal fibers, as revealed by immunocytochemical analysis at day 21.

In the presence of PDGF-AA, EGF and bFGF, hMLPCs differentiated into astrocytes and stained positively for astrocyte markers GFAP and S100, and for human markers HuNu and human specific microtubule marker. These results support a sequential model for motoneuron-glia differentiation, in which astrocytes are generated in sequential order from proliferating stem cells, after establishment of motoneurons and oligodendrocytes. It is well known that PDGF-AA, EGF and bFGF have a positive effect on stem cell proliferation. Thus, increased proliferation time could be one of the key factors responsible for astrocyte fate in this system. The responsiveness of differentiating astrocytes to NE was expected. Both astrocytes and oligodendrocytes are contacted by noradrenergic synaptic terminals and astrocytes, like oligodendrocytes, express alpha and beta adrenergic receptors.

To generate a pure population of human astrocytes, cells were separated from neurons utilizing a Percoll density gradient. After the separation, the cells were replated to produce a homogenous culture and the differentiated astrocytes exhibited large rounded cell bodies with long processes, morphologically resembling protoplasmic astrocytes. Cells were surprisingly large in size, some

reaching over 200 μm . These observations could be explained by previously published findings indicating that human protoplasmic astrocytes are approximately 2.6 times larger than their rodent counterparts^{6, 11}.

These studies demonstrated for the first time methods for obtaining human oligodendrocytes and astrocytes in high yield from human umbilical cord stem cells in defined and controllable environmental conditions. Alternative differentiation into oligodendrocytes or astrocytes was achieved entirely by environmental control. Furthermore, unlike other studies employing sonic hedgehog signaling, NE was utilized as a novel differentiation molecule and noradrenergic signaling as a novel route to attain a glial fate from adult stem cells.

Human umbilical cord stem cells are a highly promising source of cells for tissue regeneration¹⁰⁵. Compared to adult stem cells obtained from bone marrow, these cells are immature and elicit a lower incidence of graft rejection, graft-versus-host disease and low post transplant infections¹⁰⁵. Besides this biological superiority, these stem cells are abundantly available and routinely harvested without risk to the donor¹⁰⁶. Compared to embryonic stem cells, obtained from human embryos, human umbilical cord stem cells are not only easily obtainable, but also could be more suitable for cellular therapeutics. Embryonic stem cells have been associated with reports of the uncontrollable development of teratomas in a syngeneic transplantation model, imprinting-related developmental abnormalities and ethical issues. Human umbilical cord stem cells, readily available and differentiated by environmental signals, offer an added potential therapeutic advantage. These cells can be used as a source of cells for cellular therapeutics at this particularly tenuous time for embryonic stem cell research, after a federal ruling that undercut government

funding for many initiatives in the field, including Geron Corporation. Human cells obtained from umbilical cord can represent the next wave: living cells as therapeutics.

Future studies will expand understanding of the role of the microenvironmental signals and noradrenergic signaling in the glial differentiation. Terminally differentiated functional human oligodendrocytes and astrocytes will be generated for use in *in vivo* studies to develop treatment for conditions such as multiple sclerosis, neuropathy and traumatic brain injury.

LIST OF REFERENCES

1. Baumann, N. & Pham-Dinh, D. Biology of oligodendrocyte and myelin in the mammalian central nervous system. *Physiol Rev* **81**, 871-927 (2001).
2. Barkovich, A.J. Concepts of myelin and myelination in neuroradiology. *AJNR Am J Neuroradiol* **21**, 1099-1109 (2000).
3. Frankenhaeuser, B. Saltatory conduction in myelinated nerve fibres. *J Physiol* **118**, 107-112 (1952).
4. Frankenhaeuser, B. & Schneider, D. Some electrophysiological observations on isolated single myelinated nerve fibres (saltatory conduction). *J Physiol* **115**, 177-184 (1951).
5. Hirano, A. A confirmation of the oligodendroglial origin of myelin in the adult rat. *J Cell Biol* **38**, 637-640 (1968).
6. Oberheim, N.A. et al. Uniquely hominid features of adult human astrocytes. *J Neurosci* **29**, 3276-3287 (2009).
7. Volterra, A. & Meldolesi, J. Astrocytes, from brain glue to communication elements: the revolution continues. *Nat Rev Neurosci* **6**, 626-640 (2005).
8. Blackburn, D., Sargsyan, S., Monk, P.N. & Shaw, P.J. Astrocyte function and role in motor neuron disease: a future therapeutic target? *Glia* **57**, 1251-1264 (2009).
9. Araque, A., Carmignoto, G. & Haydon, P.G. Dynamic signaling between astrocytes and neurons. *Annu Rev Physiol* **63**, 795-813 (2001).
10. Valverde, F. & Lopez-Mascaraque, L. Neuroglial arrangements in the olfactory glomeruli of the hedgehog. *J Comp Neurol* **307**, 658-674 (1991).
11. Oberheim, N.A., Wang, X., Goldman, S. & Nedergaard, M. Astrocytic complexity distinguishes the human brain. *Trends Neurosci* **29**, 547-553 (2006).

12. Miller, R.H. & Raff, M.C. Fibrous and protoplasmic astrocytes are biochemically and developmentally distinct. *J Neurosci* **4**, 585-592 (1984).
13. Peters, A. & Feldman, M.L. The projection of the lateral geniculate nucleus to area 17 of the rat cerebral cortex. I. General description. *J Neurocytol* **5**, 63-84 (1976).
14. Raff, M.C., Abney, E.R., Cohen, J., Lindsay, R. & Noble, M. Two types of astrocytes in cultures of developing rat white matter: differences in morphology, surface gangliosides, and growth characteristics. *J Neurosci* **3**, 1289-1300 (1983).
15. Allen, N.J. & Barres, B.A. Neuroscience: Glia - more than just brain glue. *Nature* **457**, 675-677 (2009).
16. LeVine, S.M. & Goldman, J.E. Embryonic divergence of oligodendrocyte and astrocyte lineages in developing rat cerebrum. *J Neurosci* **8**, 3992-4006 (1988).
17. Warf, B.C., Fok-Seang, J. & Miller, R.H. Evidence for the ventral origin of oligodendrocyte precursors in the rat spinal cord. *J Neurosci* **11**, 2477-2488 (1991).
18. Noll, E. & Miller, R.H. Oligodendrocyte precursors originate at the ventral ventricular zone dorsal to the ventral midline region in the embryonic rat spinal cord. *Development* **118**, 563-573 (1993).
19. Carmen, J. et al. Revisiting the astrocyte-oligodendrocyte relationship in the adult CNS. *Prog Neurobiol* **82**, 151-162 (2007).
20. Rao, M.S., Noble, M. & Mayer-Proschel, M. A tripotential glial precursor cell is present in the developing spinal cord. *Proc Natl Acad Sci U S A* **95**, 3996-4001 (1998).
21. Rao, M.S. & Mayer-Proschel, M. Glial-restricted precursors are derived from multipotent neuroepithelial stem cells. *Dev Biol* **188**, 48-63 (1997).
22. Mayer-Proschel, M., Kalyani, A.J., Mujtaba, T. & Rao, M.S. Isolation of lineage-restricted neuronal precursors from multipotent neuroepithelial stem cells. *Neuron* **19**, 773-785 (1997).

23. Stiles, C.D. Lost in space: misregulated positional cues create tripotent neural progenitors in cell culture. *Neuron* **40**, 447-449 (2003).
24. Richardson, W.D. et al. Oligodendrocyte lineage and the motor neuron connection. *Glia* **29**, 136-142 (2000).
25. Wu, S., Wu, Y. & Capocchi, M.R. Motoneurons and oligodendrocytes are sequentially generated from neural stem cells but do not appear to share common lineage-restricted progenitors in vivo. *Development* **133**, 581-590 (2006).
26. Kippert, A., Fitzner, D., Helenius, J. & Simons, M. Actomyosin contractility controls cell surface area of oligodendrocytes. *BMC Cell Biol* **10**, 71 (2009).
27. Ohlstein, B., Kai, T., Decotto, E. & Spradling, A. The stem cell niche: theme and variations. *Curr Opin Cell Biol* **16**, 693-699 (2004).
28. Raff, M.C., Miller, R.H. & Noble, M. A glial progenitor cell that develops in vitro into an astrocyte or an oligodendrocyte depending on culture medium. *Nature* **303**, 390-396 (1983).
29. Noble, M. Precursor cell transitions in oligodendrocyte development. *J Cell Biol* **148**, 839-842 (2000).
30. Behar, T.N. Analysis of fractal dimension of O2A glial cells differentiating in vitro. *Methods* **24**, 331-339 (2001).
31. Bansal, R. & Pfeiffer, S.E. Novel stage in the oligodendrocyte lineage defined by reactivity of progenitors with R-mAb prior to O1 anti-galactocerebroside. *J Neurosci Res* **32**, 309-316 (1992).
32. Pfeiffer, S.E., Warrington, A.E. & Bansal, R. The oligodendrocyte and its many cellular processes. *Trends Cell Biol* **3**, 191-197 (1993).
33. Volpe, J.J. *Neurology of the Newborn*, Edn. 5. (Elsevier Health Sciences, 2008).

34. Ishibashi, T. et al. Astrocytes promote myelination in response to electrical impulses. *Neuron* **49**, 823-832 (2006).
35. Ffrench-Constant, C. & Raff, M.C. The oligodendrocyte-type-2 astrocyte cell lineage is specialized for myelination. *Nature* **323**, 335-338 (1986).
36. Baron, W., Metz, B., Bansal, R., Hoekstra, D. & de Vries, H. PDGF and FGF-2 signaling in oligodendrocyte progenitor cells: regulation of proliferation and differentiation by multiple intracellular signaling pathways. *Mol Cell Neurosci* **15**, 314-329 (2000).
37. Ghiani, C.A. et al. Neurotransmitter receptor activation triggers p27(Kip1) and p21(CIP1) accumulation and G1 cell cycle arrest in oligodendrocyte progenitors. *Development* **126**, 1077-1090 (1999).
38. Mokry, J. et al. Differentiation of neural stem cells into cells of oligodendroglial lineage. *Acta Medica (Hradec Kralove)* **50**, 35-41 (2007).
39. Chandran, S., Svendsen, C., Compston, A. & Scolding, N. Regional potential for oligodendrocyte generation in the rodent embryonic spinal cord following exposure to EGF and FGF-2. *Glia* **24**, 382-389 (1998).
40. Hu, H. et al. Emotion enhances learning via norepinephrine regulation of AMPA-receptor trafficking. *Cell* **131**, 160-173 (2007).
41. Tully, K. & Bolshakov, V.Y. Emotional enhancement of memory: how norepinephrine enables synaptic plasticity. *Mol Brain* **3**, 15.
42. Schildkraut, J.J. & Kety, S.S. Biogenic amines and emotion. *Science* **156**, 21-37 (1967).
43. Commissiong, J.W. Development of catecholaminergic nerves in the spinal cord of the rat. *Brain Res* **264**, 197-208 (1983).
44. Tanaka, H., Takahashi, S. & Oki, J. Developmental regulation of spinal motoneurons by monoaminergic nerve fibers. *J Peripher Nerv Syst* **2**, 323-332 (1997).

45. Rajaofetra, N., Poulat, P., Marlier, L., Geffard, M. & Privat, A. Pre- and postnatal development of noradrenergic projections to the rat spinal cord: an immunocytochemical study. *Brain Res Dev Brain Res* **67**, 237-246 (1992).
46. Laifenfeld, D., Klein, E. & Ben-Shachar, D. Norepinephrine alters the expression of genes involved in neuronal sprouting and differentiation: relevance for major depression and antidepressant mechanisms. *J Neurochem* **83**, 1054-1064 (2002).
47. Williams, N.G., Zhong, H. & Minneman, K.P. Differential coupling of alpha1-, alpha2-, and beta-adrenergic receptors to mitogen-activated protein kinase pathways and differentiation in transfected PC12 cells. *J Biol Chem* **273**, 24624-24632 (1998).
48. Paspalas, C.D. & Papadopoulos, G.C. Ultrastructural relationships between noradrenergic nerve fibers and non-neuronal elements in the rat cerebral cortex. *Glia* **17**, 133-146 (1996).
49. Khorchid, A., Cui, Q., Molina-Holgado, E. & Almazan, G. Developmental regulation of alpha 1A-adrenoceptor function in rat brain oligodendrocyte cultures. *Neuropharmacology* **42**, 685-696 (2002).
50. Khorchid, A., Larocca, J.N. & Almazan, G. Characterization of the signal transduction pathways mediating noradrenaline-stimulated MAPK activation and c-fos expression in oligodendrocyte progenitors. *J Neurosci Res* **58**, 765-778 (1999).
51. Ventimiglia, R., Greene, M.I. & Geller, H.M. Localization of beta-adrenergic receptors on differentiated cells of the central nervous system in culture. *Proc Natl Acad Sci U S A* **84**, 5073-5077 (1987).
52. Cohen, R.I. & Almazan, G. Norepinephrine-stimulated PI hydrolysis in oligodendrocytes is mediated by alpha 1A-adrenoceptors. *Neuroreport* **4**, 1115-1118 (1993).
53. Asotra, K. & Macklin, W.B. Protein kinase C activity modulates myelin gene expression in enriched oligodendrocytes. *J Neurosci Res* **34**, 571-588 (1993).
54. Bernstein, M., Lyons, S.A., Moller, T. & Kettenmann, H. Receptor-mediated calcium signalling in glial cells from mouse corpus callosum slices. *J Neurosci Res* **46**, 152-163 (1996).

55. Vartanian, T., Sprinkle, T.J., Dawson, G. & Szuchet, S. Oligodendrocyte substratum adhesion modulates expression of adenylate cyclase-linked receptors. *Proc Natl Acad Sci U S A* **85**, 939-943 (1988).
56. Dorn, G.W., 2nd, Tepe, N.M., Wu, G., Yatani, A. & Liggett, S.B. Mechanisms of impaired beta-adrenergic receptor signaling in G(alphaq)-mediated cardiac hypertrophy and ventricular dysfunction. *Mol Pharmacol* **57**, 278-287 (2000).
57. Burdick, J.A. & Vunjak-Novakovic, G. Review: Engineered Microenvironments for Controlled Stem Cell Differentiation. *Tissue Eng Part A* (2008).
58. Vogel, V. & Sheetz, M. Local force and geometry sensing regulate cell functions. *Nat Rev Mol Cell Biol* **7**, 265-275 (2006).
59. Rosenberg, S.S., Kelland, E.E., Tokar, E., De la Torre, A.R. & Chan, J.R. The geometric and spatial constraints of the microenvironment induce oligodendrocyte differentiation. *Proc Natl Acad Sci U S A* **105**, 14662-14667 (2008).
60. McBeath, R., Pirone, D.M., Nelson, C.M., Bhadriraju, K. & Chen, C.S. Cell shape, cytoskeletal tension, and RhoA regulate stem cell lineage commitment. *Dev Cell* **6**, 483-495 (2004).
61. Engler, A.J., Sen, S., Sweeney, H.L. & Discher, D.E. Matrix elasticity directs stem cell lineage specification. *Cell* **126**, 677-689 (2006).
62. Schaffner, A.E., Barker, J.L., Stenger, D.A. & Hickman, J.J. Investigation of the factors necessary for growth of hippocampal neurons in a defined system. *J Neurosci Methods* **62**, 111-119 (1995).
63. Spargo, B.J. et al. Spatially controlled adhesion, spreading, and differentiation of endothelial cells on self-assembled molecular monolayers. *Proc Natl Acad Sci U S A* **91**, 11070-11074 (1994).
64. Stenger, D.A., Pike, C.J., Hickman, J.J. & Cotman, C.W. Surface determinants of neuronal survival and growth on self-assembled monolayers in culture. *Brain Res* **630**, 136-147 (1993).

65. Varghese, K. et al. Regeneration and characterization of adult mouse hippocampal neurons in a defined in vitro system. *J Neurosci Methods* **177**, 51-59 (2009).
66. Das, M. et al. Adult rat spinal cord culture on an organosilane surface in a novel serum-free medium. *In Vitro Cell Dev Biol Anim* **41**, 343-348 (2005).
67. Settleman, J. Tension precedes commitment-even for a stem cell. *Mol Cell* **14**, 148-150 (2004).
68. Katayama, Y. et al. Signals from the sympathetic nervous system regulate hematopoietic stem cell egress from bone marrow. *Cell* **124**, 407-421 (2006).
69. Ffrench-Constant, C. & Raff, M.C. Proliferating bipotential glial progenitor cells in adult rat optic nerve. *Nature* **319**, 499-502 (1986).
70. Gross, R.E. et al. Bone morphogenetic proteins promote astroglial lineage commitment by mammalian subventricular zone progenitor cells. *Neuron* **17**, 595-606 (1996).
71. Nakashima, K. et al. BMP2-mediated alteration in the developmental pathway of fetal mouse brain cells from neurogenesis to astrocytogenesis. *Proc Natl Acad Sci U S A* **98**, 5868-5873 (2001).
72. Hughes, S.M., Lillien, L.E., Raff, M.C., Rohrer, H. & Sendtner, M. Ciliary neurotrophic factor induces type-2 astrocyte differentiation in culture. *Nature* **335**, 70-73 (1988).
73. Lillien, L.E., Sendtner, M. & Raff, M.C. Extracellular matrix-associated molecules collaborate with ciliary neurotrophic factor to induce type-2 astrocyte development. *J Cell Biol* **111**, 635-644 (1990).
74. Yoshida, T. & Takeuchi, M. Establishment of an astrocyte progenitor cell line: induction of glial fibrillary acidic protein and fibronectin by transforming growth factor-beta 1. *J Neurosci Res* **35**, 129-137 (1993).
75. Nakagaito, Y., Yoshida, T., Satoh, M. & Takeuchi, M. Effects of leukemia inhibitory factor on the differentiation of astrocyte progenitor cells from embryonic mouse cerebral hemispheres. *Brain Res Dev Brain Res* **87**, 220-223 (1995).

76. Yoshida, T., Satoh, M., Nakagaito, Y., Kuno, H. & Takeuchi, M. Cytokines affecting survival and differentiation of an astrocyte progenitor cell line. *Brain Res Dev Brain Res* **76**, 147-150 (1993).
77. Johe, K.K., Hazel, T.G., Muller, T., Dugich-Djordjevic, M.M. & McKay, R.D. Single factors direct the differentiation of stem cells from the fetal and adult central nervous system. *Genes Dev* **10**, 3129-3140 (1996).
78. Richards, L.J. et al. Leukaemia inhibitory factor or related factors promote the differentiation of neuronal and astrocytic precursors within the developing murine spinal cord. *Eur J Neurosci* **8**, 291-299 (1996).
79. Bonni, A. et al. Regulation of gliogenesis in the central nervous system by the JAK-STAT signaling pathway. *Science* **278**, 477-483 (1997).
80. Qian, X., Davis, A.A., Goderie, S.K. & Temple, S. FGF2 concentration regulates the generation of neurons and glia from multipotent cortical stem cells. *Neuron* **18**, 81-93 (1997).
81. Wang, S. & Barres, B.A. Up a notch: instructing gliogenesis. *Neuron* **27**, 197-200 (2000).
82. Lillien, L.E., Sendtner, M., Rohrer, H., Hughes, S.M. & Raff, M.C. Type-2 astrocyte development in rat brain cultures is initiated by a CNTF-like protein produced by type-1 astrocytes. *Neuron* **1**, 485-494 (1988).
83. Hickman, J.J. et al. Rational Pattern Design for in-Vitro Cellular Networks Using Surface Photochemistry. *J. Vac. Sci. Technol. A-Vac. Surf. Films* **12**, 607-616 (1994).
84. Brewer, G.J. Isolation and culture of adult rat hippocampal neurons. *J Neurosci Methods* **71**, 143-155 (1997).
85. Das, M. et al. Auto-catalytic ceria nanoparticles offer neuroprotection to adult rat spinal cord neurons. *Biomaterials* **28**, 1918-1925 (2007).
86. Das, M. et al. Embryonic motoneuron-skeletal muscle co-culture in a defined system. *Neuroscience* **146**, 481-488 (2007).

87. Lu, Q.R. et al. Common developmental requirement for Olig function indicates a motor neuron/oligodendrocyte connection. *Cell* **109**, 75-86 (2002).
88. Pringle, N.P. et al. Determination of neuroepithelial cell fate: induction of the oligodendrocyte lineage by ventral midline cells and sonic hedgehog. *Dev Biol* **177**, 30-42 (1996).
89. Takashima, Y. et al. Neuroepithelial cells supply an initial transient wave of MSC differentiation. *Cell* **129**, 1377-1388 (2007).
90. Miller, F.D. Riding the waves: neural and nonneural origins for mesenchymal stem cells. *Cell Stem Cell* **1**, 129-130 (2007).
91. Ravenscroft-Chang, M.S. et al. Altered calcium dynamics in cardiac cells grown on silane-modified surfaces. *Biomaterials* **31**, 602-607.
92. Wright, C.D. et al. Nuclear alpha1-adrenergic receptors signal activated ERK localization to caveolae in adult cardiac myocytes. *Circ Res* **103**, 992-1000 (2008).
93. Huang, Y. et al. An alpha1A-adrenergic-extracellular signal-regulated kinase survival signaling pathway in cardiac myocytes. *Circulation* **115**, 763-772 (2007).
94. Raible, D.W. & McMorris, F.A. Oligodendrocyte differentiation and progenitor cell proliferation are independently regulated by cyclic AMP. *J Neurosci Res* **34**, 287-294 (1993).
95. Casaccia-Bonnel, P. & Liu, A. Relationship between cell cycle molecules and onset of oligodendrocyte differentiation. *J Neurosci Res* **72**, 1-11 (2003).
96. Billon, N., Jolicoeur, C., Tokumoto, Y., Vennstrom, B. & Raff, M. Normal timing of oligodendrocyte development depends on thyroid hormone receptor alpha 1 (TRalpha1). *EMBO J* **21**, 6452-6460 (2002).
97. Weinstein, D.E. Isolation and purification of primary rodent astrocytes. *Curr Protoc Neurosci* **Chapter 3**, Unit 3 5 (2001).

98. Masahira, N. et al. Olig2-positive progenitors in the embryonic spinal cord give rise not only to motoneurons and oligodendrocytes, but also to a subset of astrocytes and ependymal cells. *Dev Biol* **293**, 358-369 (2006).
99. van de Ven, C., Collins, D., Bradley, M.B., Morris, E. & Cairo, M.S. The potential of umbilical cord blood multipotent stem cells for nonhematopoietic tissue and cell regeneration. *Exp Hematol* **35**, 1753-1765 (2007).
100. Izrael, M. et al. Human oligodendrocytes derived from embryonic stem cells: Effect of noggin on phenotypic differentiation in vitro and on myelination in vivo. *Mol Cell Neurosci* **34**, 310-323 (2007).
101. Rogister, B., Ben-Hur, T. & Dubois-Dalcq, M. From neural stem cells to myelinating oligodendrocytes. *Mol Cell Neurosci* **14**, 287-300 (1999).
102. Nguyen, L. et al. The Yin and Yang of cell cycle progression and differentiation in the oligodendroglial lineage. *Ment Retard Dev Disabil Res Rev* **12**, 85-96 (2006).
103. Raible, D.W. & McMorris, F.A. Cyclic AMP regulates the rate of differentiation of oligodendrocytes without changing the lineage commitment of their progenitors. *Dev Biol* **133**, 437-446 (1989).
104. Bhat, N.R., Zhang, P. & Mohanty, S.B. p38 MAP kinase regulation of oligodendrocyte differentiation with CREB as a potential target. *Neurochem Res* **32**, 293-302 (2007).
105. El-Badri, N.S. et al. Cord blood mesenchymal stem cells: Potential use in neurological disorders. *Stem Cells Dev* **15**, 497-506 (2006).
106. Kogler, G. et al. A new human somatic stem cell from placental cord blood with intrinsic pluripotent differentiation potential. *J Exp Med* **200**, 123-135 (2004).